Front. Earth Sci. 2016, 10(3): 455–478
DOI 10.1007/s11707-016-0577-0

RESEARCH ARTICLE

# Late Quaternary rates of stream incision in Northeast Peloponnese, Greece

**Efthimios KARYMBALIS (✉)[1], Dimitrios PAPANASTASSIOU[2], Kalliopi GAKI-PAPANASTASSIOU[3], Maria FERENTINOU[4], Christos CHALKIAS[1]**

1 Department of Geography, Harokopio University, Athens 17671, Greece
2 Institute of Geodynamics, National Observatory of Athens, Athens 11810, Greece
3 Department of Geography and Climatology, Faculty of Geology and Geoenvironment, National and Kapodistrian University of Athens, Athens 15784, Greece
4 Department of Geology, School of Agricultural, Earth and Environmental Sciences, University of KwaZulu-Natal, Westville Campus, Private Bag X54001, Durban 4000, South Africa



**Abstract** This study focuses on defining rates of fluvial incision for the last 580±5 kyr along valley systems of eight streams that drain the eastern part of the northern Peloponnese. The streams are developed on the uplifted block of the offshore-running Xylokastro normal fault, one of the main faults bounding the southern edge of the Gulf of Corinth half-graben, and have incised a set of ten uplifted marine terraces having an amphitheatric shape. These terraces range in age from 60±5 kyr to 580±5 kyr and have been mapped in detail and correlated with late Pleistocene oxygen-isotope stages of high sea-level stands by previous studies. The terraces were used in this paper as reference surfaces in order to define fluvial incision rates at the lower reaches of the studied streams. To evaluate incision rates, thirty-three topographic valley cross-sections were drawn using fieldwork measurements as well as using a highly accurate (2×2 cell size) Digital Elevation Model (DEM) at specific locations where streams cut down the inner edges of the marine terraces. For each cross-section the ratio of valley floor width to valley height (Vf) and long-term mean stream incision rates were estimated for the last 580±5 kyr, while rock uplift rates were estimated for the last 330±5 kyr. The geomorphic evolution of the valleys on the uplifted block of the Xylokastro fault has been mainly driven by the lithology of the bedrock, sea level fluctuations during the late Quaternary, and incision of the channels due to the tectonic uplift. Stream incision rates range from 0.10±0.1 mm/yr for the last 123±7 kyr to 1.14±0.1 mm/yr for the last 310±5 kyr and are gradually greater from east to west depending on the distance from the trace of the fault. Downcutting rates are comparable with the rock uplift rates, which range from 0.4±0.02 mm/yr to 1.49±0.12 mm/yr, over the last 330±5 kyr.

**Keywords** fluvial incision, tectonic uplift, marine terraces, Peloponnese, Greece

Received September 19, 2015; accepted December 15, 2015

E-mail: karymbalis@hua.gr

## 1 Introduction

The landscape in actively deforming areas results from interactions between tectonic uplift or subsidence and consequent surface processes that can lead to local erosion or deposition. The estimation of rates and relative contributions of each process at a particular time or over some span of time are very useful in order to understand the evolution of the landscape in tectonically active areas (Burbank and Anderson, 2007; Finnegan et al., 2008). Moreover, a landscape's morphology can provide insights into the interactions of surface processes and uplift. In tectonically active settings characterized by long-term uplift, river incision rates are strongly dependent on the rates of uplift (e.g., Seong et al., 2008). As the capacity of a river to incise bedrock and transport sediments depends on channel gradient, a positive feedback exists between bedrock uplift and river incision (Whipple and Tucker, 1999). Relief is therefore thought to evolve toward a dynamic equilibrium between uplift and downcutting (Wakabayashi and Sawyer, 2001; Whipple, 2001; Kirby and Whipple, 2012). Such equilibrium is often assumed and used in neotectonic studies to infer uplift rates from river incision rate measurements (e.g., Merritts and Vincent, 1989; Harbor, 1998; Leland et al., 1998; Lavé and Avouac, 2001; Syndera et al., 2003).

Many studies around the world focus on defining rates of

fluvial incision along river valley systems from mapping and dating of fill terraces or strath terraces' abandonment (among others Leland et al., 1998; Pazzaglia and Brandon, 2001; Brocard et al., 2003; Proença Cunha et al., 2005; Seong et al., 2008; Carcaillet et al., 2009). Moreover, there are studies concerning the evolution of fluvial systems in uplifting coastal areas in different tectonic environments where the fluvial response to uplift rates is examined by dating the timing of marine terrace abandonment (e.g., Merritts and Bull, 1989, for California; Kraal, 1999, for Costa Rica; Rostami et al., 2000, for Argentinean Patagonia; Zazo et al., 2003, for Spain; Marquardt et al., 2004, for Chile; Cucci, 2004, for the Calabrian arc in Italy; Pillans, 1990, for New Zealand and many others). In many tectonically active coastal areas characterized by the presence of uplifted marine terraces the evolution of the landscape is affected by fault activity (Corbi et al., 2009; Robustelli et al., 2009a). Many studies investigate the role of contemporaneous fault activity and the distance from major faults that can locally modify the uplift rates affecting the efficiency of land surface processes (including fluvial incision) and long term topographic development (Robustelli et al., 2009b).

Marine terraces are generally erosional or thin depositional platforms that slope seawards very gently ($\leqslant 10°$). They have a landward margin, or inner edge marked by the shoreline angle at the base of the coeval palaeo-sea cliff and a seaward eroded edge at the top of the next, younger sea cliff. A series of such platforms and cliffs resembles a flight of stairs carved into the coastal topography. Inner edges of the terraces are therefore precise markers of abandoned marine shorelines, formed horizontally, at sea-level (Armijo et al., 1996; Maroukian et al., 2008; Gaki-Papanastassiou et al., 2009). Marine or lake strandlines are generally good markers to define palaeo-horizontal planes, as they correspond to a base level at the time of their formation. Thus, a marine terrace of known age and elevation above present sea-level can be used to compute a rate of bedrock uplift (Burbank and Anderson, 2007).

The principle objective of this study is to define rates of long-term fluvial incision for the last $580\pm5$ kyr along the valley systems of eight streams (Trikalitikos, Katharoneri, Seliandros, Elisson, Assopos, Zapantis, Raizanis, and Xerias), that drain an area of 838.3 $km^2$ of the tectonically uplifting area of northeastern Peloponnese in central Greece (Fig. 1). The study area lies in the uplifting block of the Xylokastro fault, which is one of the main south bounding faults of the Gulf of Corinth (also called the Corinth rift). A series of ten well preserved uplifted marine terraces, which have been correlated with the worldwide chronology of glacio-eustatic sea-level highstands in the last 580 kyr (Armijo et al., 1996), were used as reference surfaces for the estimation of long-term channel incision rates at thirty-three locations where streams cut through the terraces. Furthermore, long-term rock uplift rates for various time intervals were extracted from the terraces. Several papers have been published about this area, using the raised geomorphic features to evaluate uplift rates for the causative faults. However there are no studies concerning the estimation of incision rates in space and time and the evolution of the valley profiles. This paper analyzes both spatial and temporal variations of incision rates in this area and explores the relationship between tectonic and erosional processes. The relation between fluvial downcutting and the shape of the valleys is investigated by correlating long-term mean incision rates with the ratio of valley floor width to valley height (Vf) values and estimating the appropriate equation. Additionally, the relationship between channel incision values and the distance to the Xylokastro fault trace as well as the correlation between the shape of the valley (Vf values) and the distance from the fault were examined.

## 2 The study area

The Gulf of Corinth is an N 100°E oriented, elongated (150 km long) asymmetric half-graben, with an uplifted southern coast and downward flexed northern one, separating Peloponnese from Central Greece. It started to form about 3.2 – 3.0 Ma (Leeder et al., 2012). It is characterized by high levels of seismicity and extension rates which are higher in the western part of the Gulf, about 14 mm/yr, decreasing towards the east reaching 13 mm/yr in the center and 10 mm/yr in the east (Rigo et al., 1996; Ambraseys and Jackson, 1997; Clarke et al., 1998; Briole et al., 2000; Avallone et al., 2004; Floyd et al., 2010; Chousianitis et al., 2013). It communicates with the open Ionian Sea on the west through the Rion–Antirion straits having a maximum depth of 65 m. At the east end the Corinth rift bifurcates into two sub-basins, the Alkyonides Gulf and the Lechaion Gulf, separated by the Perachora peninsula (Fig. 1). The Lechaion Gulf with its exhumed southern margins is not considered to be part of the active rift but of a proto-Gulf of Corinth (Turner et al., 2010).

Almost all of the focal mechanisms and surface ruptures in the Gulf of Corinth correspond to normal faulting, with an extension roughly N-S oriented (Jackson et al., 1982, Stewart, 1996; Pavlides and Caputo, 2004). This is consistent with the overall rift structure, which is outlined by a prominent topographic depression with an ~ ESE-WNW direction across the NNW-SSE trending fabric of the Hellenic mountain belt. The large normal faults that bound the rift cut the fold-thrust tectonic units of the belt, which consist mainly of Mesozoic and Tertiary phyllites, ophiolites, unmetamorphosed flysch formations, and thick platform carbonates (IGME, 1983).

A series of three main en echelon active, roughly E-W trending, normal fault segments (Psathopyrgos, Heliki, and Xylokastro faults) bound the high relief along the southern coast and enter the sea in the east (Fig. 1) cutting the fold-thrust tectonic units of the Hellenic belt (Doutsos and

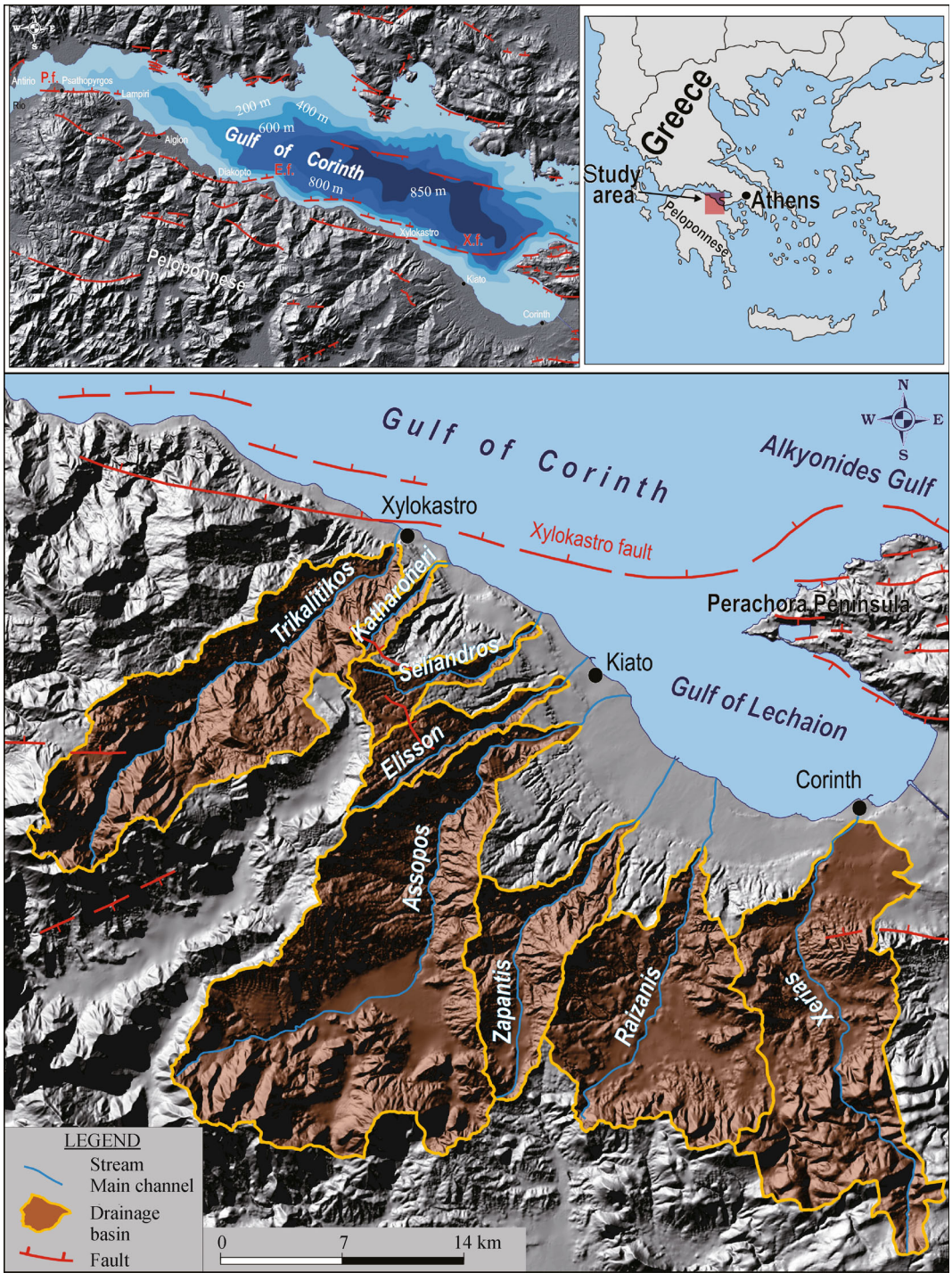


**Fig. 1** Hill shade maps of the Gulf of Corinth and the studied streams' catchments. The main faults of the Gulf of Corinth are also depicted (P.f.: Psathopyrgos fault; E.f.: Eliki fault; X.f.: Xylokastro fault).

Piper, 1990; Armijo et al., 1996; Bell et al., 2009). Active faulting on the southern side of the Gulf has resulted in Pleistocene uplift of the mountains in the south where the study area is located. The streams of the study area drain the uplifting footwall of the offshore extension of the Xylokastro normal fault, which is one of the major faults bounding the south coast of the Gulf of Corinth half-graben (Fig. 1). According to Armijo et al. (1996) the motion on the Xylokastro fault started 1 Ma ago and its maximum uplift rate is on the order of 1.3 mm/yr, while a slip rate of 6 – 7 mm/yr over the last 350 kyr is proposed. This rate appears to be 10 times faster than that for comparable features in the area (Koukouvelas et al., 2005).

The southern coast of the Gulf is characterized by a series of raised geomorphic features, like marine terraces, Gilbert fan deltas, tilted surfaces, and drainage reversals

that uplifted during the late Quaternary due to the activity of the faults that bound the coast (Armijo et al., 1996; Morewood and Roberts, 1999; McNeill and Collier, 2004; Leeder et al., 2005; Rohais et al., 2008; Palyvos et al., 2010; Ford et al., 2013). This activity continues today as the uplifted marine notches, beach rocks, and archaeological remnants show (Papageorgiou et al., 1993; Stewart and Vita-Finzi, 1996; Maroukian et al., 1997; Kershaw and Guo, 2001; Pirazzoli et al., 2004). South of the Gulf of Corinth normal faults with attitudes very similar to those at the present rift edge occur. They generally lack clear morphological evidence of young activity. Both the seismicity and the morphology suggest that these faults are older (of early Quaternary age) and less active, than the faults at the present rift edge (Armijo et al., 1996). This indicates that both the normal fault activity and the southern edge of the evolving Corinth rift have migrated northwards.

Among all the uplifted geomorphic features of the southern coast, the most impressive and extensive one is the flight of ten marine terraces, developed in a NW-SE direction, with an amphitheatric shape, ranging in elevation from 10 to 400 m, which lie on the footwall of the above mentioned E-W striking Xylokastro normal fault (Fig. 2). The terraces are close to the Xylokastro fault at the western part of the study area but they move away (up to 40 km) from the fault, towards the east. These terraces have been cut in a region of relatively modest topography (Fig. 2) which corresponds to the dominant occurrence in the former Gulf of thick, soft marls, which are mainly freshwater lacustrine to brackish facies and of loosely determined Plio-Pleistocene age (Freyberg, 1973; Sebrier, 1977; Collier, 1990) interbedded with some marine marls and shoreface sands and conglomerates.

Marine fossil assemblages suggest that part of the marls is of middle to late Pleistocene age (Keraudren and Sorel, 1987). Each terrace comprises an erosion-resistant lid of caprock generally 2–6 m thick formed from well-cemented sands and conglomerates. Many authors have studied these marine platforms using morphological and sedimentological observations and have tried to distinguish and correlate them in space and time (Deperet, 1913; Sebrier, 1977; Dufaure and Zamanis, 1980; Vita-Finzi and King, 1985; Keraudren and Sorel, 1987; Doutsos and Piper, 1990; Armijo et al., 1996; Westeway, 2002).

Detail mapping of the terraces together with proper use

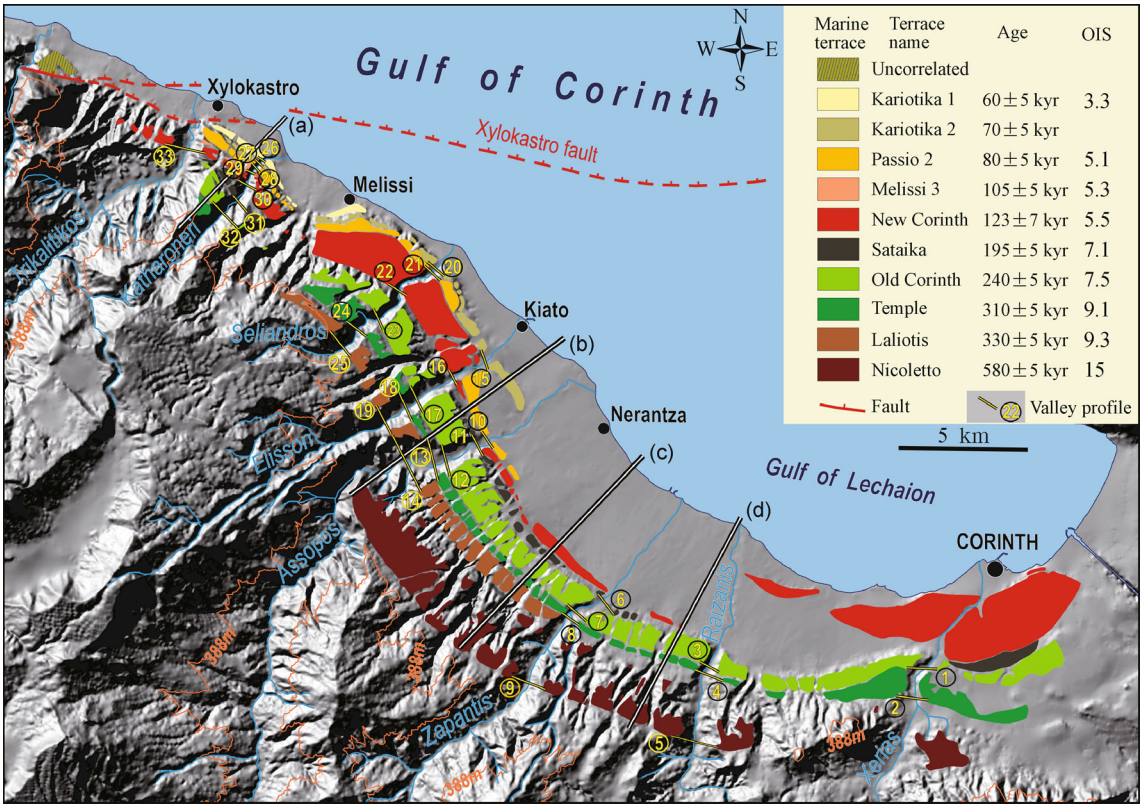


**Fig. 2** Hill shade map of the broader area of the uplifted marine terraces between Corinth and Xylokastro. The locations of the valley-cross profiles, which were used for the estimations of mean long-term fluvial incision rates and ratio of valley floor width to valley height values, are also indicated. Hill shade map is produced by topographic maps at the scale of 1:50,000. Locations of the four cross-sections ((a), (b), (c), and (d) in Fig. 3) at different distances from the Xylokastro fault are indicated. Marine terraces and faults are based on Armijo et al. (1996).

of the absolute sea-level variations led Armijo et al. (1996) to revise the views of the previous researchers while accepting that the processes involved in the formation of the terraces are essentially the same. Based on detailed mapping of the terraces, supported by stratigraphic evidence and existing U/Th dates, they correlated these platforms with highstand sea-level stages of the oxygen-isotope chronology (e.g., Chappell and Shackleton, 1986) and deduced rates of tectonic uplift. Thus, they correlated the most prominent marine platforms with very high sea-level stands and ascribed an oxygen-isotope stage to each one of the other terraces (Fig. 3). The most prominent and continuous terraces in the Corinth – Xylokastro area are the New Corinth and the Old Corinth. They are thus good candidates to correspond to very high sea-level stands, similar to the present interglacial.

The stratigraphic and palaeontological evidence suggests that the New Corinth terrace corresponds to the Tyrrhenian (Sebrier, 1977). This is the stratigraphic level with the typical fauna association with *Strombus bubonius*, generally correlated with the last interglacial, isotopic stage 5.5 (Eutyrrhenian ≈124 kyr) (Vita-Finzi and King, 1985; Valensise and Pantosti, 1992). Samples of mollusks collected at about 20 m gave U/Th dates of 49±20 kyr

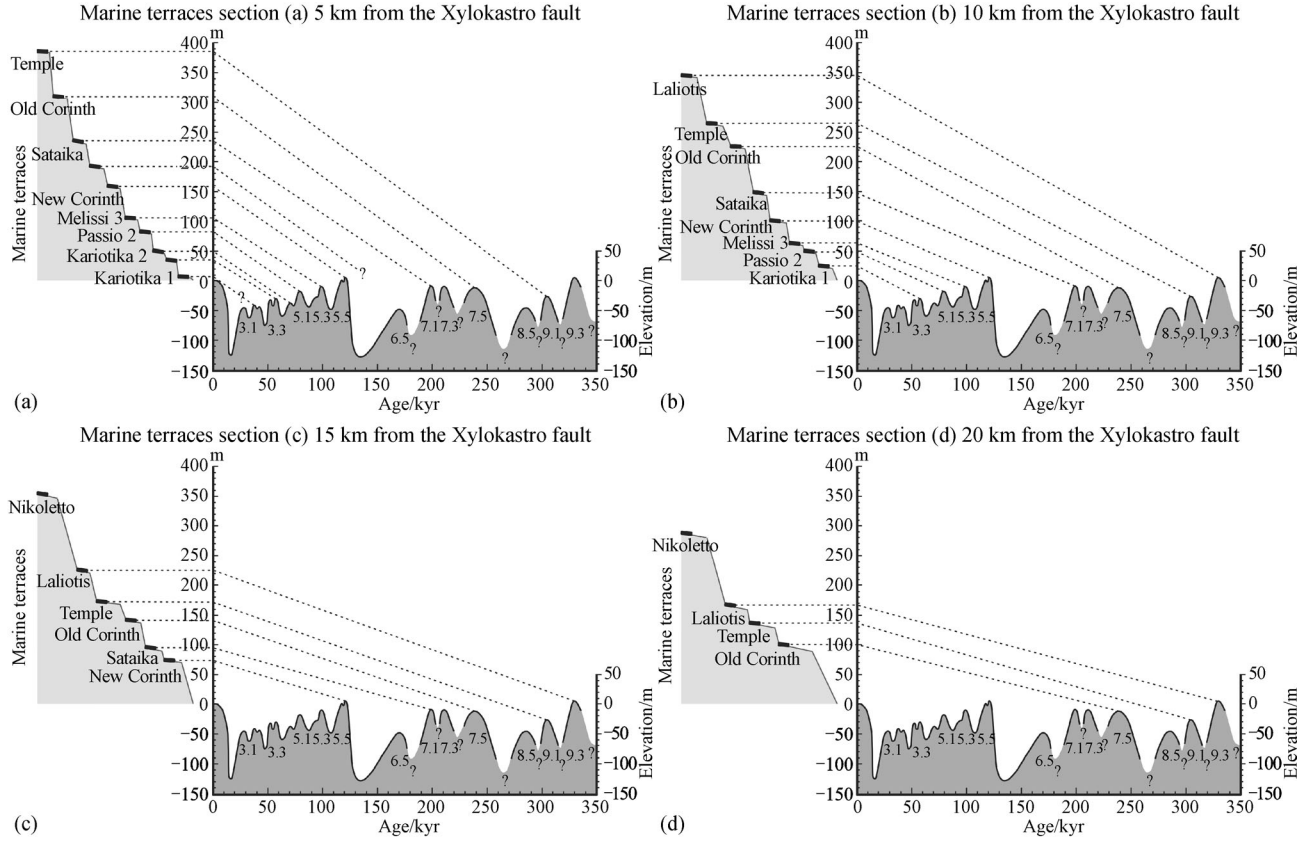


**Fig. 3** Correlation of marine terraces in space and time. The elevations of palaeo-shorelines at four sections at different distances from the Xylokastro fault (5, 10, 15, and 20 km) are correlated with the sea-level highstands (modified from Armijo et al. (1996)). Locations of the four sections ((a), (b), (c), and (d)) are indicated in Fig. 2.

**Table 1** Characteristics of the streams and their corresponding drainage basins

| Stream | Length of the main channel/km | Total channels length/km | Basin area/km$^2$ | Drainage density | Basin slope/% |
|---|---|---|---|---|---|
| Xerias | 32.2 | 341.5 | 164.7 | 2.07 | 25 |
| Raizanis | 24.1 | 299.4 | 135.6 | 2.21 | 25 |
| Zapantis | 25.2 | 190.5 | 66.47 | 2.87 | 33 |
| Assopos | 45.2 | 555.5 | 268.4 | 2.07 | 32 |
| Elisson | 17.9 | 77.23 | 27.95 | 2.76 | 35 |
| Seliandros | 15.1 | 53.94 | 21.47 | 2.51 | 29 |
| Katharoneri | 7.8 | 44.11 | 14.69 | 3.00 | 44 |
| Trikalitikos | 32.1 | 403.20 | 139.0 | 2.90 | 44 |

(Sebrier, 1977). For the Old Corinth terrace, the U/Th dating of mollusk shells gives an age of 235 kyr (+40, −30) (Sebrier, 1977). Two U/Th analyses of the same coral sample (*Acropora* sp.) taken from the Old Corinth terrace 3 km south of the city of Corinth yields dates of 232 kyr (+23.6, −19,7) and of 177 kyr (+11.0, −10.1), which differ at the 1σ level (Collier et al., 1992). U/Th dating of another coral sample (*Cladocora caespitosa*) collected southwest of Corinth gave an age of 132.1±8.2 kyr (Leeder et al., 2003). Clearly, these absolute ages are inaccurate and insufficient. Taking them at their face value, however, these ages suggest that the Old Corinth terrace may well correlate with isotope stage 7. With neither absolute dates nor good corals to sample, which is a common obstacle in many places of the world, Armijo et al. (1996) used a simple technique which assumes a nearly constant uplift rate at each locality on the coastline. This approach is particularly adapted to assess the ages of the Pleistocene shorelines in the Xylokastro-Corinth area because their 3D geometry is accurately constrained. They correlated the Kariotika 1 terrace with OIS 3.3 having an age of 60 kyr, Kariotika 2 with the 70 kyr OIS, Passio 2 with OIS 5.1 at 80 kyr, Melissi 3 with OIS 5.3 at 105 kyr, New Corinth with OIS 5.5 at 123 kyr, Sataika with OIS 7.1 at 195 kyr, Old Corinth with OIS 7.5 at 240 kyr, Temple with OIS 9.1 at 310 kyr, Laliotis with OIS 9.3 at 330 kyr, and Nikoletto with OIS 15.1 at 580 kyr (Fig. 2). In our study we follow this correlation in space and time proposed by Armijo et al. (1996) since it is the only one existing until today and well accept by the scientific community (Figs. 2 and 3). Additionally, we use the local names of marine terraces given by the same authors.

Concerning the climatic conditions of the area, north Peloponnese experiences a typical Mediterranean climate with annual temperatures averaging 15°C. The mean annual precipitation ranges between 550 mm in the northern low-lying coastal area and 700 mm in the southern mountainous region (Katsafados et al., 2009). Rainfall is distributed relatively unevenly with about 75% of it occurring between the months of October and March. Given the small area of the study and the similarity in physical setting from E-W, the precipitation can be

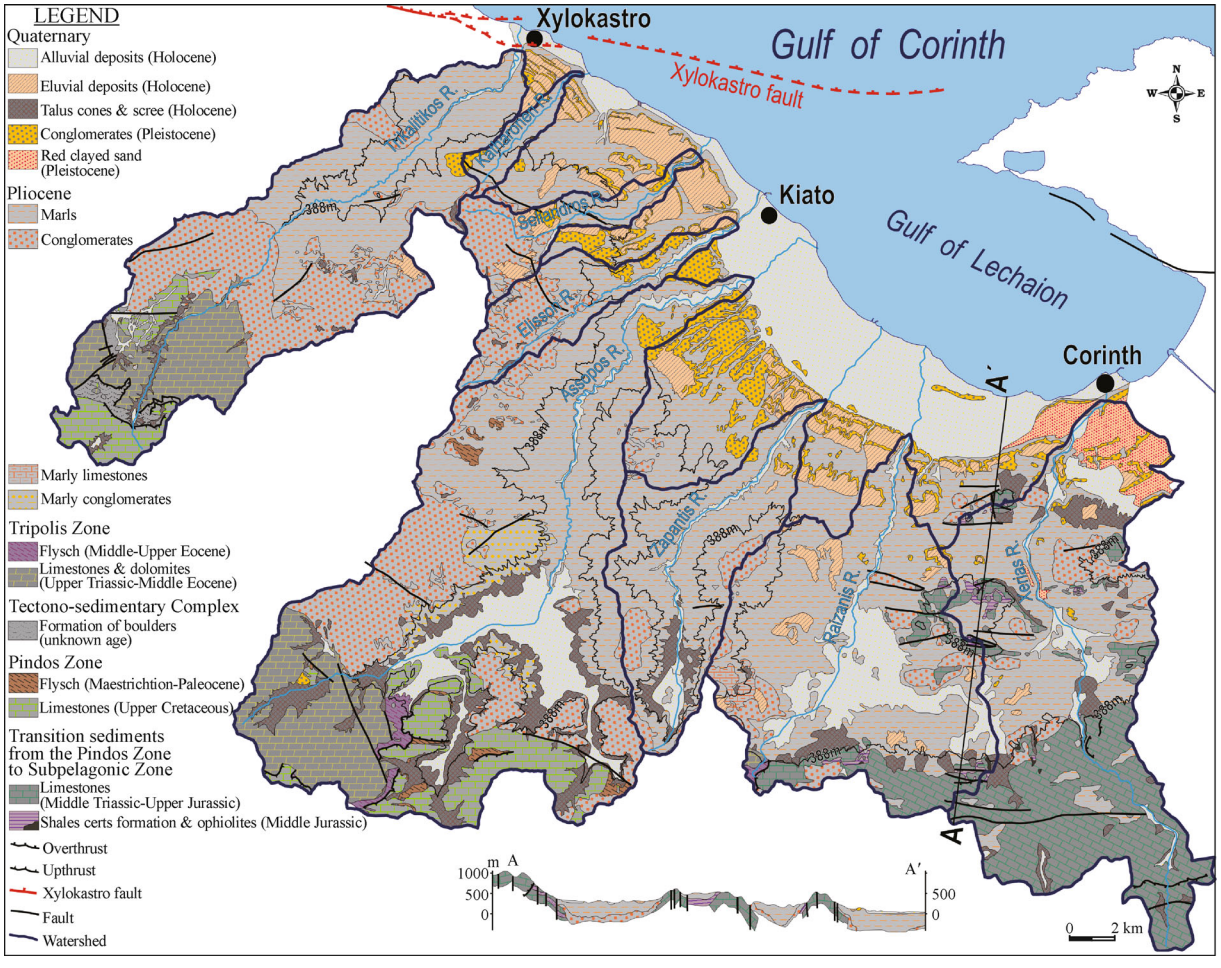


**Fig. 4** Geological map of the drainage basins (based on the geological mapping by the Institute of Geology and Mineral Exploration of Greece at a scale of 1:50,000, (IGME, 1970, 1972, 1982, 1989). A geological cross-section (A–A′) is also included. The location of the cross-section is shown on the map.

presumed to be fairly similar in each drainage basin. Most of the streams are of seasonal flow and the lengths of their main channels range between 7.8 km (Katharoneri stream) and 45.2 km (Assopos stream). They flow from SSW to NNE and discharge into the Gulf of Corinth along the coastline between the cities of Corinth and Xylokastro (Fig. 1). The drainage basins range in area from 14.69 km$^2$ (Katharoneri catchment) to 268.4 km$^2$ (Assopos catchment) (Table 1). The southern part of the more extensive catchments of Xerias, Raizanis, Assopos, and Trikalitikos consists of Mesozoic age geological formations resistant to erosion (mainly limestones, but also dolomites and flysch layers which belong to the geotectonic zones of Gavrovo-Tripolis, Olonos-Pindos, and the transition formations from the Pindos to Subpelagonic zone) (IGME, 1970, 1972, 1982, 1989). The northern part of the drainage basins is dominated by late Pliocene less resistant fluvial and lacustrine sands, silts, and conglomerates, passing upwards to Quaternary marls and conglomerates (Fig. 4). The small catchments of Zapantis, Elisson, Seliandros, and Katharoneri streams are exclusively developed on these weak Plio-Pleistocene formations on which the above mentioned marine terraces have been cut. Consequently it is assumed that these small drainage basins are similar in terms of erodibility, whereas the larger basins have a less erodible upper part.

## 3 Methods and data used

To evaluate the fluvial incision rates on the uplifted block of the Xylokastro fault we constructed thirty-three topographic valley-cross sections perpendicular to the main channels of the rivers at specific locations where streams cut down the uplifted marine terraces along their lower reaches. The cross sections have been drawn by combined fieldwork measurements and use of a 2×2 cell size DEM produced by detailed topographic diagrams (at the scale of 1:5,000) with a good contour density (4 m contour interval, as well as 1 m in some specific relatively flat regions) which cover the study area, obtained from the Hellenic Military Geographical Service. The DEM covers an area of 42.5 km$^2$ (~10.6 million pixels) and its horizontal and vertical mean square errors are 2 m. The site of each one of the thirty-three topographic cross sections was selected as close as possible to the morphologically defined slope break angle, which marks a marine terrace's inner edge, because these points correspond precisely to the age of the palaeo-shoreline during the interglacial stage. The accuracy of the determination of the palaeo-shoreline angle elevations is quite good as the vertical uncertainty due to both the vertical mislocation error of the inner edge and the vertical standard mean square error on the DEM used is less than ±2 m. These marine platforms allow the reconstruction of the geometry and age of the former, prior to the formation of the valley-surface that represents the hypothesized topography in the absence of erosion, so bedrock incision can be directly calculated. In order to estimate fluvial downcutting, the present shape of the terraces, which is the result of stream incision, is compared with a curve that approximates their initial surface. Our estimates do not cover areas with elevation greater than 388 m, due to the lack of marine terraces upstream from this point. Rock uplift rates have also been estimated for the locations of the valley-cross topographic sections.

The investigation of the morphology and the shape of the valleys include the measurement of various morphometric characteristics from the valley-cross topographic profiles of the thirty-three locations along the main stream channels. These indices include the width (Vw) and the height (Vh) of the valley, the ratio of valley width and valley height (Vw/Vh), the width of valley floor (Vfw), the elevations of the valley floor (Esc) as well as of the left and right divides (Eld, Erd), and the ratio of valley floor width to valley height (Vf). Vf was calculated using the following formula (Bull and McFadden, 1977):

$$\mathrm{Vf} = \mathrm{Vfw}/[(\mathrm{Eld}-\mathrm{Esc}) + (\mathrm{Erd}-\mathrm{Esc})/2],$$

where Vfw = the width of valley floor, Eld = the elevation of the left drainage divide, Erd = the elevation of the right drainage divide, and Esc = the elevation of the valley floor.

Vf is the most indicative index of the form or shape of the valley cross-section and describes the degree of maturity of the valley. It is also a parameter that helps to define V-shaped deep valleys which may be associated with rapid uplift (Bull and McFadden, 1977). Thus it is a good measure that indicates whether the river is actively downcutting and incising (Bull and McFadden, 1977; Kale and Shejwalkar, 2008).

The uncertainties for the calculated ratio of valley floor width to valley height (Vf) values are mainly associated with the accuracy of the 2×2 cell size DEM. An uncertainty of ±1 m for the elevations of the left and the right drainage divides (Eld and Erd respectively), which correspond to the elevation of the marine terrace's inner edge, is taken into account, while an additional error of ±1 m due to mislocation of the inner edges' elevation (Eld and Erd) was included. Therefore the total average uncertainty in elevation estimates of shoreline angles is ±2 m. Moreover uncertainties of ±1 m for the elevation of the valley floor and of ±2 m for the width of the valley floor are also included.

In a tectonically active area, the shape of a valley profile is commonly linked to the rate of uplift. The higher the rate of uplift, the more incised the valley cross-section profile. Hence, small values of Vf reflect deep, narrow, V-shaped valleys which are commonly associated with regions of relatively rapid uplift. In contrast, high values are markers of wide, open valleys in regions of minimal uplift rates as valley width increases with time due to lateral migration and erosion (Keller and Pinter, 1996).

Stream incision is the change in elevation between the inner edge of the marine terrace and the level of the modern stream channel. Since the inner edge represents the topography at the time of terrace formation, and the abandonment age of each marine platform is known, the long-term stream incision rate can be evaluated. It can be estimated by measuring the elevation difference between the present channel and the tops of caprock deposits and dividing the elevation difference by the age of the marine terrace. Taking into account the ages of the terraces, it was possible to estimate the time-average incision rates for the eight streams in the northeastern part of the Peloponnese for various time periods from 580±5 kyr ago until recent times. In order to extract the rock uplift rates we identified the elevation of the inner edge of the marine terrace for each location of the valley-cross profiles. The elevation of the inner edge of the terraces allows the precise estimation of the amount of uplift from the given elevation of sea-level at the time of their formation. Hence the elevations of the inner edges were corrected according to the respective sea-level stand in relation to present sea-level (Fig. 3). The long-term rock uplift rate was evaluated by dividing the corrected elevation of the inner edge by the age of the marine terrace. We did not estimate uplift rates for the highest terrace (Nikoletto −580±5 kyr) because little is known of sea-level positions during the interglacial periods older than OIS 11 and the correction of the elevation of the inner edge was quite difficult (Murray-Wallace and Woodroffe, 2014). For both long-term incision and rock uplift rate estimates, we took into consideration uncertainties that include: a measurement error of ±2 m for the elevation of the inner edge and of ±1 m for the elevation of the valley floor associated with the accuracy of the 2×2 cell size DEM and uncertainties associated with the age of marine terraces (±5 kyr for all of the terraces and ±7 kyr for the terrace which corresponds to the OIS 5.5) since the palaeoshoreline does not represent a specific age but the duration of the highstands (Turner et al., 2010). These errors are typically greater than the age analysis uncertainty. Our estimates on both valley morphology and incision do not cover areas with elevations greater than 388 m for which the long-term average incision rates are likely to be higher, due to the lack of marine terraces upstream from this point. Furthermore, they do not give a measure of the downcutting in the most resistant rocks of the pre-Neogene Alpine basement. In this way both spatial and temporal distribution of Vf values and incision rates along the lower reaches of the studied streams were reconstructed for the last 580±5 kyr. The variation of Vf values, fluvial incision rates, and rock uplift rates as a function of the distance of the valleys from the Xylokastro fault trace was also explored.

In an attempt to investigate the response of the study streams to the tectonic uplift as well as to the fluctuations of the eustatic sea-level during the late Pleistocene period, the longitudinal profiles of the main stream channels were constructed and analyzed using a DEM (20 m×20 m) derived from 1:50,000 scale topographic maps of the Hellenic Military Geographical Service covering the drainage basins' area. The horizontal and vertical standard mean square error of this DEM was 15 m and 10 m respectively.

Additionally, in order to estimate the potential erosive power of overland flows (as well as its local inequalities) for the channels under investigation, the stream power (i.e., the energy of a stream at specific point) was estimated at the locations of the valley-cross profiles along the main streams channels. Stream power was estimated by using the Stream Power Index (SI). This index is directly related to the stream power if we assume that discharge is directly proportional to upslope contributing area (CA). This assumption is valid for small basins/watersheds, such as the catchments of the study area (Seong et al., 2008). Another operating assumption is that the geology is consistent in the drainage basins. Although erodibility has a major impact on incision/aggradation, the Stream Power Index (SI) does not take into consideration the geology of the catchment. Another geologic factor within watersheds that may influence stream power is sediment transport since above a certain threshold sediment-load-transported sediment works against stream power. The Stream Power Index (SI) used in this study takes into account the local slope geometry and the site location in the basin, combining data on slope gradient and catchment area (Florinsky, 2012). The index is calculated as:

$$\mathrm{SI} = \log(\mathrm{CA} * \tan G)$$

where CA and $G$ are catchment area and slope gradient, respectively.

The energy slope $G$ is derived from the 2 m×2 m cell size DEM of the area. The CA is the specific catchment area (i.e., the upslope contributing area) estimated using the flow accumulation algorithm from the standard GIS-based Hydrology toolbox. For this estimation the (20 m×20 m) DEM was used since the detailed DEM was available only for the northern part of the study area and do not cover the entire drainage basins' area.

## 4 Results

### 4.1 Longitudinal profiles

The longitudinal profiles of the streams are indicative of a gradual decrease in uplift magnitude eastward (Fig. 5). The channels of the small streams in the west part of the area (Elisson, Seliandros, and Katharoneri) are very steep. Trikalitikos River, the westernmost of the streams, has a lower gradient profile, at least along its lower reaches, mainly due to the higher discharge since it drains a much more extensive area. For a given rate of uplift, smaller streams will be steeper in order to maintain the power

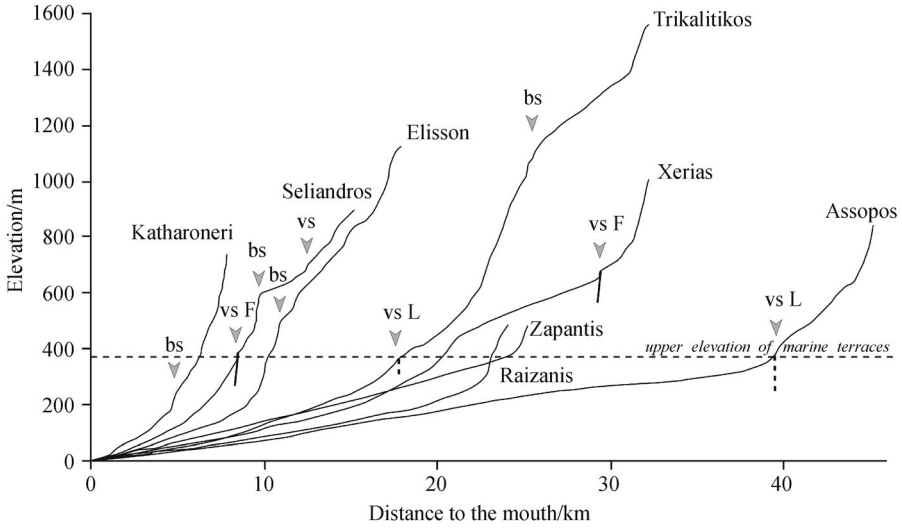


**Fig. 5** Longitudinal profiles of the eight rivers, derived from (20 m×20 m) DEM produced by 1:50,000 scale topographic maps of the Hellenic Military Geographical Service. The positions of the major knickpoints within each river profile are also depicted. Bold lines represent faults producing surface displacements, whereas dashed lines represent the lithologic boundaries associated with knickpoints. (bs: break slope knickpoints, vs: vertical step knickpoints, F: main faults affecting the longitudinal profiles, L: lithologic contacts).

necessary to incise vertically at a rate similar to that of the uplift rate (Merritts et al., 1994). Rapid uplift in this area is attributed to its proximity to the trace of the Xylokastro fault (Fig. 1). On the other hand the streams of the east part of the area, which are far away from the fault, have more concave longitudinal profiles and significantly lower channel slopes due to the lower uplift rates of no more than 0.3 mm/yr which characterize the Corinth plain (Collier et al., 1992; Armijo et al., 1996; McNeill and Collier, 2004; Turner et al., 2010; Demoulin et al., 2015).

The knickpoints along the steams' main channels can be divided into two groups: vertical-step knickpoints and break slope knickpoints (Haviv et al., 2010; Kirby and Whipple, 2012; Demoulin et al., 2015). Break slope knickpoints are located 5.1 km (elevation: 260 m), 9.8 km (elevation 600 m), 11.3 km (elevation: 520 m) and 26.0 km (elevation: 1140 m) upstream from the mouths of Katharoneri, Seliandros, Elisson, and Trikalitikos, respectively. These knickpoints separate reaches that are in equilibrium with previous conditions (above the knickpoint) and the current conditions (below the knickpoint).

At the upper reaches of some of the streams are found vertical-step knickpoints, associated principally with discrete heterogeneities along the profiles. Two vertical-step knickpoints located 29.4 km (elevation: 680 m) and 8.4 km (elevation: 380 m) upstream from the mouths of Xerias and Seliandros respectively, are the result of normal faults (Figs. 4 and 5). These two faults are less active than the those of the present Corinth rift edge. The fault of the upper reaches of Xerias cuts through limestones while the fault of Seliandros cuts marls. Thus the erodibility on either side of the faults is the same. The knickpoint at the upper reaches of the Assopos River is associated with the lithologic boundary of hard to erode rocks of Palaeozoic age with less resistant Plio-Pleistocene formations, while a knickpoint 17.6 km upstream from the Trikalitikos River mouth coincides with a change in channel lithology from relatively resistant conglomerates to less resistant marls (Fig. 5). The lower reaches of the streams lack any occurrence of significant knickpoints. This can be attributed to the highly erodible lithology (mainly marls) along the channels of the northern part of the study area.

### 4.2 Ratio of valley floor width to valley height (Vf)

Valley form and long-term fluvial incision rates are dependent on bedrock lithology, tectonics, and surface process dynamics. All cross-valley profiles were constructed at locations consisting of almost the same lithology, marls of Plio-Pleistocene age, capped by relatively resistant, well-cemented sands and conglomerates which correspond to the surfaces of the marine terraces (Fig. 6). Consequently, for all eight studied streams, bedrock lithology affects valley morphology and stream incision in a rather similar way.

Table 2 includes the values of the valley's morphometric parameters measured from the valley-cross sections (Fig. 6). As already mentioned, for each of the selected streams the requisite valley width and height data were obtained along multiple valley cross sections drawn perpendicular to the main stream channels. Vf values within the study area range between 0.10±0.01 and 13.00±2.49 and vary significantly between different locations. The lower value corresponds to the valley

**Table 2** Values of the morphometric parameters of the valleys for each valley-cross profile drawn along the main channels of the rivers. Stream Power Index (SI), mean rock uplift rates, and mean incision rates for each location are also included

| Cross-valley profile number | Stream | Time range /kyr | Valley width (Vw) /m | Valley height (Vh) /m | Vw/Vh | Width of valley floor (Vfw)/m | Elevation of the left divide (Eld) /m | Elevation of the right divide (Erd) /m | Elevation of the valley floor (Esc) /m | Ratio of valley floor width to valley height (Vf) | Stream power index (Si) | Cumulative incision/m | Incision rate /(mm·yr$^{-1}$) | Uplift rate /(mm·yr$^{-1}$) |
|---|---|---|---|---|---|---|---|---|---|---|---|---|---|---|
| 1 | Xerias | 240±5 | 630±2 | 36.35±3 | 17.3±1.5 | 128±2 | 96±2 | 76±2 | 49.5±1 | 3.51±0.35 | 6.11 | 36 | 0.15±0.02 | 0.40±0.02 |
| 2 | Xerias | 310±5 | 800±2 | 31±3 | 25.8±2.6 | 455±2 | 108±2 | 86±2 | 61±1 | 12.64±1.12 | 6.15 | 31 | 0.10±0.01 | 0.40±0.01 |
| 3 | Raizanis | 240±5 | 550±2 | 60±3 | 9.1±0.5 | 240±2 | 100±2 | 96±2 | 39.5±1 | 4.10±0.25 | 5.90 | 60 | 0.25±0.02 | 0.45±0.02 |
| 4 | Raizanis | 310±5 | 760±2 | 80±3 | 9.5±0.4 | 219±2 | 124±2 | 120±2 | 42±1 | 2.74±0.13 | 6.11 | 81 | 0.26±0.01 | 0.48±0.01 |
| 5 | Raizanis | 580±5 | 1450±2 | 159±3 | 9.1±0.2 | 163±2 | 220±2 | 228±2 | 66±1 | 1.03±0.03 | 6.10 |  | 0.27±0.02 |  |
| 6 | Zapantis | 195±5 | 369±2 | 17±3 | 21.7±4.1 | 221±2 | 80±2 | 80±2 | 63±1 | 13.00±2.49 | 5.97 | 18 | 0.09±0.02 | 0.43±0.02 |
| 7 | Zapantis | 240±5 | 570±2 | 35,5±3 | 16.1±1.4 | 287±2 | 112±2 | 108±2 | 75.5±1 | 8.32±0.79 | 5.97 | 36 | 0.15±0.02 | 0.50±0.02 |
| 8 | Zapantis | 310±5 | 570±2 | 59,5±3 | 9.6±0.5 | 199±2 | 140±2 | 140±2 | 80.5±1 | 3.34±0.20 | 5.94 | 59 | 0.19±0.01 | 0.54±0.01 |
| 9 | Zapantis | 580±5 | 1200±2 | 165±3 | 7.3±0.1 | 294±2 | 280±2 | 276±2 | 114±1 | 1.79±0.05 | 5.95 |  | 0.28±0.02 |  |
| 10 | Assopos | 105±5 | 435±2 | 22.5±3 | 19.3±2.7 | 299±2 | 56±2 | 52±2 | 31±1 | 13.00±1.81 | 6.25 | 22 | 0.21±0.04 | 0.74±0.05 |
| 11 | Assopos | 195±5 | 425±2 | 67.5±3 | 6.3±0.3 | 257±2 | 108±2 | 102±2 | 36±1 | 3.72±0.19 | 6.25 | 68 | 0.35±0.02 | 0.56±0.02 |
| 12 | Assopos | 240±5 | 920±2 | 113.5±3 | 8.1±0.2 | 333±2 | 164±2 | 156±2 | 46.5±1 | 2.93±0.10 | 6.25 | 113 | 0.47±0.02 | 0.71±0.02 |
| 13 | Assopos | 310±5 | 1390±2 | 146±3 | 9.5±0.2 | 282±2 | 208±2 | 180±2 | 42±1 | 1.86±0.05 | 6.25 | 146 | 0.47±0.02 | 0.71±0.02 |
| 14 | Assopos | 330±5 | 1900±2 | 192±3 | 9.9±0.2 | 605±2 | 260±2 | 240±2 | 58±1 | 3.15±0.06 | 6.24 | 191 | 0.58±0.02 | 0.78±0.02 |
| 15 | Elisson | 80±5 | 550±2 | 16±3 | 34.4±6.8 | 83±2 | 52±2 | 50±2 | 34±1 | 4.88±1.01 | 5.68 | 16 | 0.20±0.05 | 0.88±0.08 |
| 16 | Elisson | 123±7 | 335±2 | 24.5±3 | 13.7±1.8 | 239±2 | 84±2 | 84±2 | 59.5±1 | 9.76±1.30 | 5.67 | 25 | 0.20±0.04 | 0.65±0.05 |
| 17 | Elisson | 240±5 | 815±2 | 100±3 | 8.2±0.3 | 211±2 | 204±2 | 184±2 | 91±1 | 2.05±0.08 | 5.68 | 101 | 0.42±0.02 | 0.85±0.03 |
| 18 | Elisson | 310±5 | 810±2 | 121±3 | 6.7±0.2 | 327±2 | 244±2 | 208±2 | 99±1 | 2.57±0.08 | 5.68 | 121 | 0.39±0.02 | 0.76±0.02 |
| 19 | Elisson | 330±5 | 730±2 | 154±3 | 4.7±0.1 | 190±2 | 280±2 | 268±2 | 119±1 | 1.23±0.04 | 5.69 | 155 | 0.47±0.02 | 0.86±0.02 |
| 20 | Seliandros | 80±5 | 560±2 | 37.5±3 | 14.9±0.3 | 165±2 | 64±2 | 60±2 | 22.5±1 | 4.18±0.37 | 5.51 | 38 | 0.47±0.07 | 1.00±0.09 |
| 21 | Seliandros | 105±5 | 465±2 | 53±3 | 8.8±0.5 | 84±2 | 88±2 | 76±2 | 26±1 | 1.50±0.12 | 5.67 | 53 | 0.50±0.05 | 1.00±0.07 |
| 22 | Seliandros | 123±7 | 255±2 | 59.5±3 | 4.3±0.3 | 58±2 | 126±2 | 108±2 | 53.5±1 | 0.91±0.07 | 5.72 | 59 | 0.48±0.05 | 0.92±0.07 |
| 23 | Seliandros | 240±5 | 505±2 | 136±3 | 3.7±0.1 | 28±2 | 228±2 | 240±2 | 100±1 | 0.21±0.02 | 5.85 | 137 | 0.57±0.02 | 1.02±0.03 |
| 24 | Seliandros | 310±5 | 730±2 | 160±3 | 4.6±0.1 | 28±2 | 300±2 | 280±2 | 130±1 | 0.18±0.02 | 5.78 | 161 | 0.52±0.02 | 1.02±0.02 |
| 25 | Seliandros | 330±5 | 970±2 | 186±3 | 5.2±0.1 | 27±2 | 388±2 | 350±2 | 174±1 | 0.14±0.01 | 5.92 | 185 | 0.56±0.02 | 1.15±0.02 |
| 26 | Katharoneri | 60±5 | 157±2 | 22.5±3 | 7.0±1.0 | 15±2 | 52±2 | 44±2 | 24.5±1 | 0.64±0.17 | 5.14 | 23 | 0.38±0.08 | 1.25±0.14 |
| 27 | Katharoneri | 70±5 | 212±2 | 37.5±3 | 5.7±0.5 | 20±2 | 68±2 | 64±2 | 28±1 | 0.53±0.09 | 5.63 | 38 | 0.54±0.08 | 1.44±0.13 |
| 28 | Katharoneri | 80±5 | 329±2 | 60.5±3 | 5.4±0.3 | 44±2 | 100±2 | 100±2 | 39.5±1 | 0.73±0.07 | 5.63 | 61 | 0.76±0.09 | 1.49±0.12 |
| 29 | Katharoneri | 105±5 | 325±2 | 84.5±3 | 3.9±0.2 | 43±2 | 132±2 | 132±2 | 47.5±1 | 0.51±0.04 | 5.46 | 84 | 0.80±0.07 | 1.49±0.09 |
| 30 | Katharoneri | 123±7 | 660±2 | 106±3 | 6.2±0.2 | 29±2 | 176±2 | 184±2 | 74±1 | 0.27±0.03 | 5.35 | 106 | 0.86±0.07 | 1.43±0.10 |
| 31 | Katharoneri | 195±5 | 620±2 | 143±3 | 4.3±0.1 | 29±2 | 240±2 | 228±2 | 93±1 | 0.21±0.02 | 5.45 | 142 | 0.73±0.03 | 1.22±0.04 |
| 32 | Katharoneri | 240±5 | 1130±2 | 200±3 | 5.7±0.1 | 19±2 | 316±2 | 298±2 | 115±1 | 0.10±0.01 | 5.37 | 199 | 0.83±0.03 | 1.33±0.04 |
| 33 | Trikalitikos | 123±7 | 1010±2 | 159±3 | 6.4±0.1 | 180±2 | 180±2 | 188±2 | 26±1 | 1.14±0.03 | 6.18 | 160 | 1.29±0.10 | 1.46±0.10 |

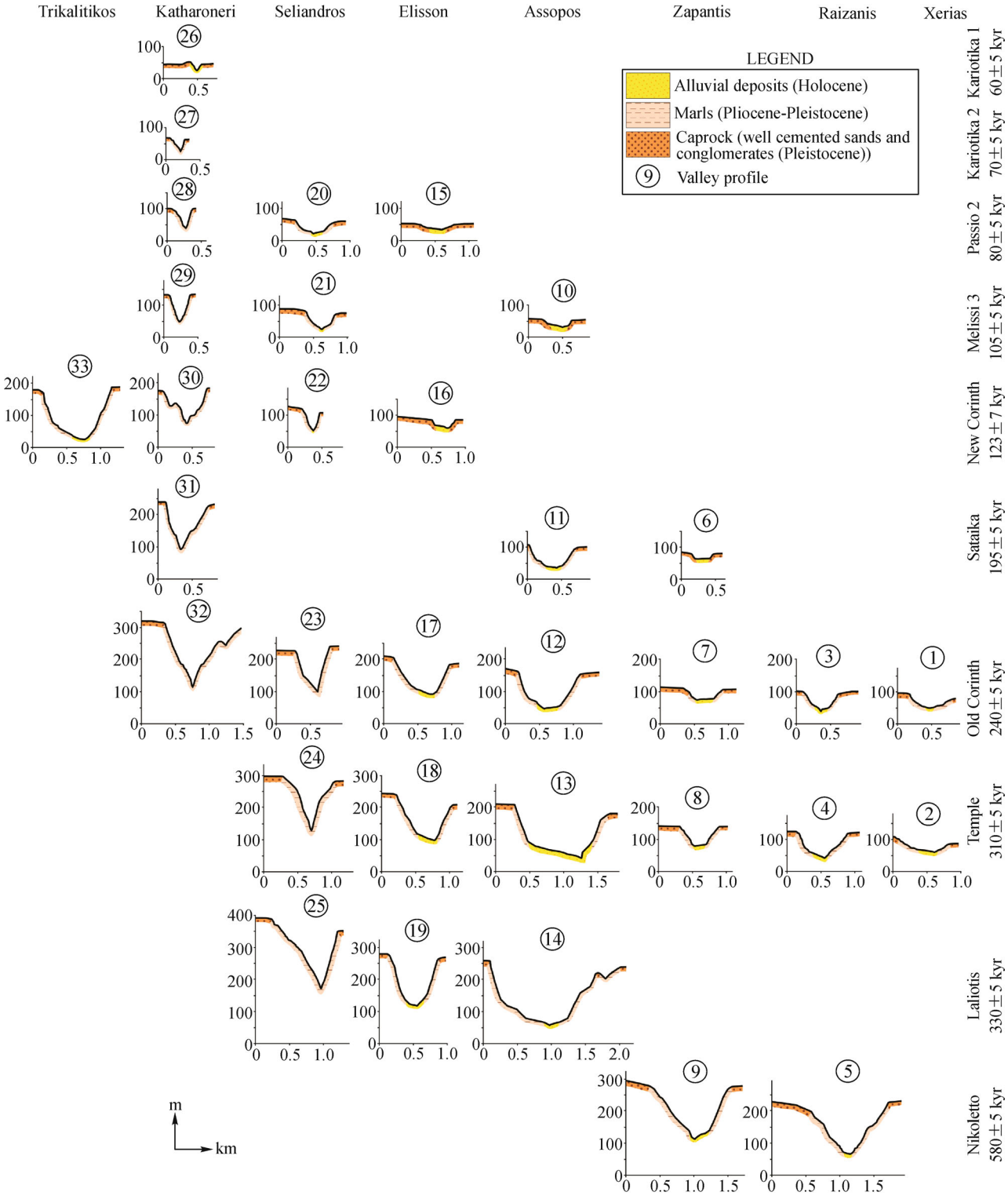


**Fig. 6** Cross-valley profiles at specific locations where the main channels of the rivers cut down the inner edges of the uplifted marine terraces. Cross-valley profiles were constructed using the 2×2 cell size DEM derived from detailed topographic diagrams (at a scale of 1:5,000) obtained from the Hellenic Military Geographical Service. These topographic profiles were used for calculating Vf values and mean stream incision rates. The lithology of the valley sides and valley floor is based on geological maps at a scale of 1:50,000 of the Institute of Geology and Mineral Exploration of Greece. The names of the streams as well as the names and age ranges of the marine terraces are indicated. The age of the incised uplifted palaeo-surface for each cross valley profile is the age of the corresponding marine terrace. The locations of the valley-cross sections are depicted in Fig. 2.

cross section of Katharoneri, which is one of the western-most streams of the study area, whereas the highest values are observed for Zapantis (Sataika terrace, 195±5 kyr, valley-cross section) and Assopos (Melissi 3, 105±5 kyr, valley-cross section), both located at the central part of the area. All valley-cross profiles of the Katharoneri stream and four of the five profiles of the Seliandros stream have Vf values less than 1.00 indicating an area experiencing rapid uplift. In general, the valleys of the Trikalitiko, Katharoneri, and Seliandros rivers are relatively narrower than the valleys of the other streams which drain the eastern part of the area (Table 2, Fig. 6). On the other hand the Vf values for the rivers of the eastern part of the study area are significantly higher than ratios of the western river valleys.

Examination of the data indicates that for almost all of the streams Vf values gradually lessen with distance upstream (Figs. 7–10). Thus, the upper reaches of the streams, which downcut gradually higher (i.e., older) marine terraces, have relatively narrower valleys in comparison to the downstream valleys of the younger marine terraces. The higher Vf values for the lower reaches of the stream valleys imply predominance of gentler, broad-floored, U-shaped valleys of relatively reduced incision. The fact that few to no alluvial deposits or well-developed fluvial terraces occur along the main channels of the streams of the western part of the study area indicates that erosion there is dominantly vertical (Merritts et al., 1994). The main valley formation factor is channel incision.

The diagram in Fig. 11 depicts the variation of Vf as a function of distance from the Xylokastro fault trace and shows clearly that the geographic distribution of Vf ratios for the same terrace are controlled by the distance of the sample sites (locations of cross-valley sections) from the fault. The correlation coefficient is relatively good (+ 0.56) and the equation describing this relation is the following:

$$\mathrm{Vf} = 0.32 * \text{distance to Xylokastro fault (km)} + 0.42$$

Higher values which imply deeper, narrower, V-shaped valleys characterize streams which are located closer to the fault whereas streams far away from the fault trace have formed relatively broad-floored, U-shaped valleys of reduced incision.

### 4.3 Long-term channel incision rates

A preliminary estimation of the erosion of the uplifted block of the Xylokastro fault has been conducted by Armijo et al. (1996). They compared the present shape of the three main terraces of the area, those of OIS 5.5, 7.5, and 9.3, incised by streams and river valleys, with a curve that approximates their initial surface. The mean erosional percentage of the three terraces is 11%, 17%, and 33% respectively. This technique gave a first approximation of the erosion in this area. We took this as an initial point. We expanded it and estimated in this work precise quantitative fluvial erosion rates for every terrace, not only for given ages but also for different distances from the fault as each terrace extends from the Xylokastro fault towards the east.

As mentioned above all cross-valley profiles were constructed at locations of almost the same lithology (marls capped by well-cemented sands and conglomerates). The streams have cut down through the caprock and the underlying marls. Most of the streams' channels flow on recent alluvial sediments except for the Katharoneri and Seliandros streams. These cut down into marls.

The calculated long-term fluvial incision rates range from 0.09±0.02 to 1.29±0.10 mm/yr (Table 2, Fig. 12). The highest rate has been estimated along the Trikalitikos stream for the post-New Corinth terrace period (post 123±7 kyr) whereas the lower fluvial incision rate is recorded along the Xerias river for the post-Temple terrace period (post 310±5 kyr) (Table 2). For any given stream, long-term channel incision generally decreases downstream, since older, higher marine terraces include the accumulated tectonic uplift compared with the newer formed lower terraces (Figs. 7–10). It is very difficult to compare fluvial incision rates measured over different time intervals. River incision is an unsteady process disturbed by episodes of reduced downcutting or deposition. Rate data estimated from different time intervals do not provide the sufficient condition because process rates are, in fact, a function of the measured time interval (Gardner et al., 1987; Finnegan et al., 2014; Gallen et al., 2015). To avoid the spurious correlation that arises from plotting a rate against its own denominator (measurement interval), we computed the power law relationship between cumulative bedrock incision and measurement interval for each of the streams (Fig. 13). Scatter plots of the data show a significant positive association between cumulative incision and time interval, although regression lines fit to the data are slightly different for each stream. For all of the streams the slope of the regression line is greater than 1 indicating a general increase in fluvial incision rate with an increase in measurement interval.

Incision is strongly controlled by the distance of the stream valleys from the active normal fault of Xylokastro (Fig. 12), as evidenced by the value of the correlation coefficient obtained (−0.74). The equation that describes the relationship is:

$$\text{Incision rate (mm/yr)} = 0.79 - 0.04 * \text{distance to Xylokastro fault (km)}$$

In general for each one of the considered periods, higher rates are observed for the Trikalitikos, Katharoneri,

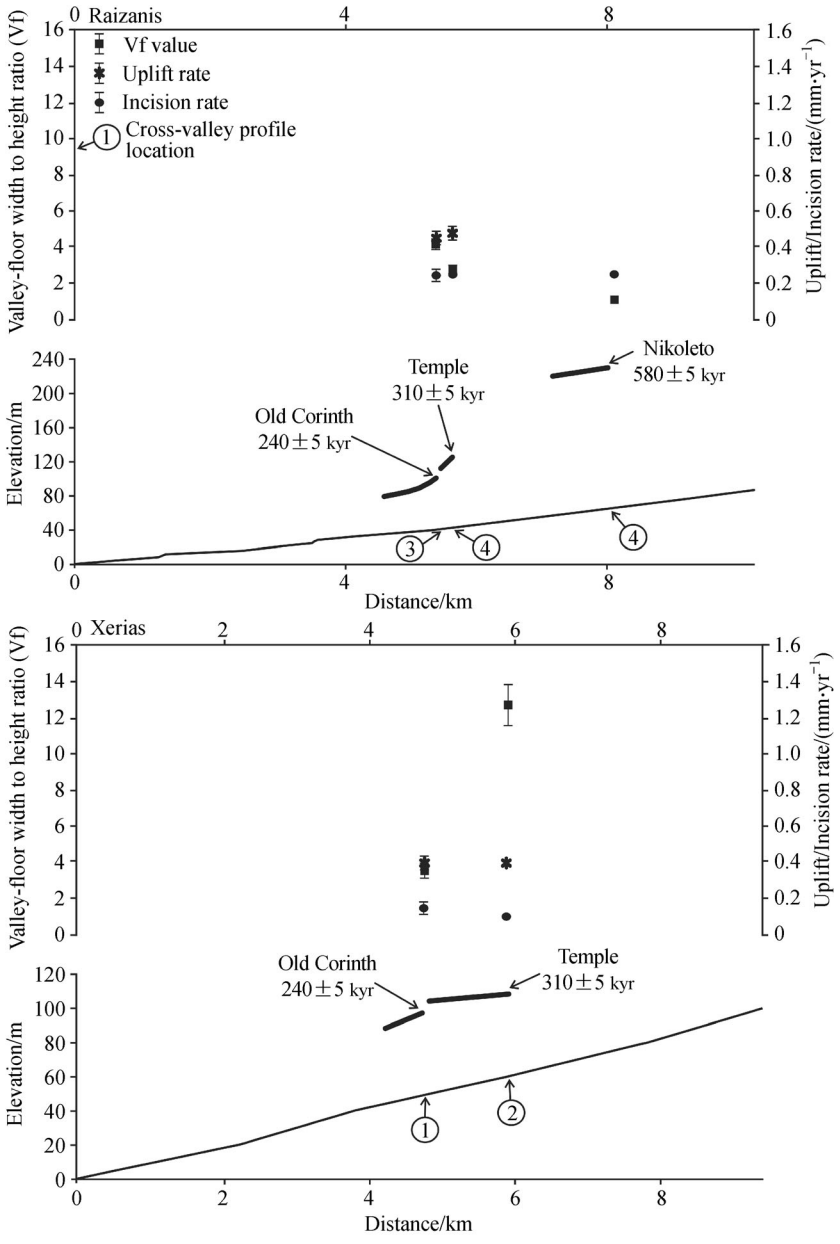


**Fig. 7** Longitudinal profiles of the lower reaches of modern Xerias and Raizanis stream beds. Profiles of marine terrace surfaces along the west bank of the stream channels are also depicted. Stream and terrace long profiles derived from (2×2 cell size) DEM produced by 1:5,000 scale topographic maps of the Hellenic Military Geographical Service. The name and the age of each marine terrace are given. Arrows indicate the locations of the inner edges of the marine terraces. Numbers in circles correspond to the locations and the numbers of the valley-cross profiles of Fig. 6 used for the estimation of long-term stream incision rates. Diagrams above longitudinal profiles show rock uplift rates, the ratio of valley floor width to valley height (Vf), and fluvial incision rates for the streams estimated from the valley-cross profiles. Right axis is the calculated uplift and incision rates; left axis is the parameter of valley floor width to valley height (Vf).

Seliandros, Elisson, and Assopos streams whereas lower incision rates were estimated for the eastern streams (Zapantis, Raizanis, and Xerias). The estimated incision rates along the main stream channels of the Seliandros, Elisson, Raizanis, and Zapantis suggest a long-term relative stability of river incision rates over the last 580±5 kyr (Figs. 7 and 9). Incision rates along Xerias, Assopos, Elisson, and Seliandros streams show a lowering of mean downcutting rate for the terrace of 310±5 kyr (Table 2, Figs. 8 and 10). A possible reason for this, as it is proved by visual inspection, is the presence on top of this platform of a more erosion resistant, thicker, and harder caprock, consisting of well cemented sands and conglomerates.

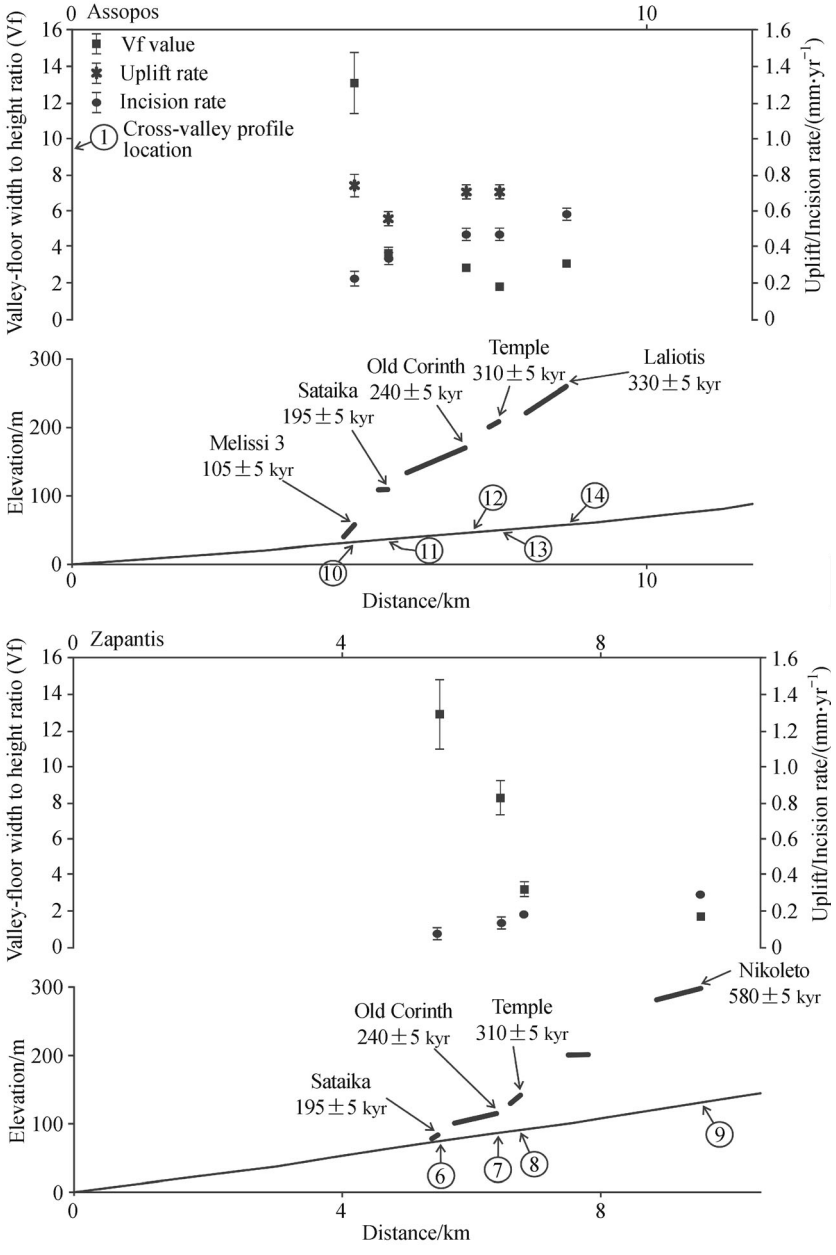


**Fig. 8** Longitudinal profiles of the lower reaches of the modern Zapantis and Assopos stream beds. Profiles of marine terrace surfaces along the west bank of the stream channels are also depicted. The name and the age of each marine terrace are given. Arrows indicate the locations of the inner edges of the marine terraces. Numbers in circles correspond to the locations and the numbers of the valley-cross profiles of Fig. 6 used for the estimation of long-term stream incision rates. Diagrams above longitudinal profiles show rock uplift rates, the ratio of valley floor width to valley height (Vf), and fluvial incision rates for the streams estimated from the valley-cross profiles. Right axis is the calculated uplift and incision rates; left axis is the parameter of valley floor width to valley height (Vf).

The estimated downcutting values correspond to mean incision rates during multiple climate cycles. The streams experienced base-level fluctuations of several tens of meters during glacial and interglacial periods. Lowering of base level during glacial periods may have accelerated the incision; on the other hand interglacial epochs must have been periods of slow incision since tectonic uplift was the only cause of downcutting. Given the fact that the Gulf of Corinth is a closed gulf which communicates with the Ionian Sea through the Rio–Antirio straits (65 m maximum depth), during glacial periods the Gulf was disconnected from the open sea and functioned as a lake. This implies that the effect of base level fluctuations during glacial periods was not as intense as for other coastal areas which were exposed to open sea. Episodes of valley incision have been mainly controlled by the footwall uplift of the

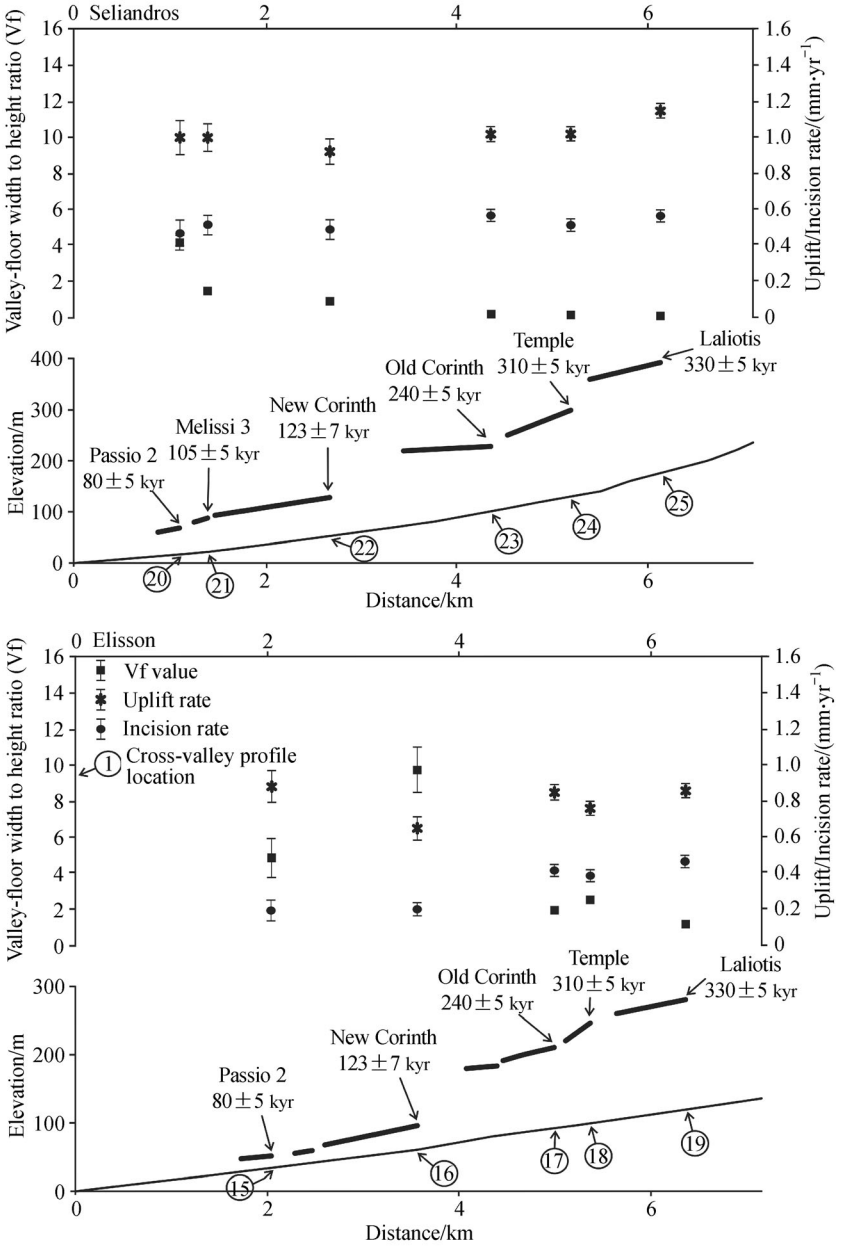


**Fig. 9** Longitudinal profiles of the lower reaches of the modern Elisson and Seliandros stream beds. Profiles of marine terrace surfaces along the west bank of the stream channels are also depicted. The name and the age of each marine terrace are given. Arrows indicate the locations of the inner edges of the marine terraces. Numbers in circles correspond to the locations and the numbers of the valley-cross profiles of Fig. 6 used for the estimation of long-term stream incision rates. Diagrams above longitudinal profiles show rock uplift rates, the ratio of valley floor width to valley height (Vf), and fluvial incision rates for the streams estimated from the valley-cross profiles. Right axis is the calculated uplift and incision rates; left axis is the parameter of valley floor width to valley height (Vf).

Xylokastro fault as well as by other local factors such as the climate, changes of base-level, and the easily erodible lithology of the area. The geographic distribution of incision rates imply that footwall uplift is the main control of the valley incision episodes identified for these streams.

There is a strong relationship between stream down-cutting and the shape of the valleys. The plot of long-term average fluvial incision rates vs. the ratio of valley floor width to valley height (Vf) is indicative of this negative, relatively good relationship (correlation coefficient: −0.63) (Fig. 14). The equation that connects these two variables has the following form:

$$\text{Incision rate (mm/yr)} = 0.59 - 0.045 * \text{Vf}$$

This association exists partly due to the lithological similarities of the geological formations along the lower

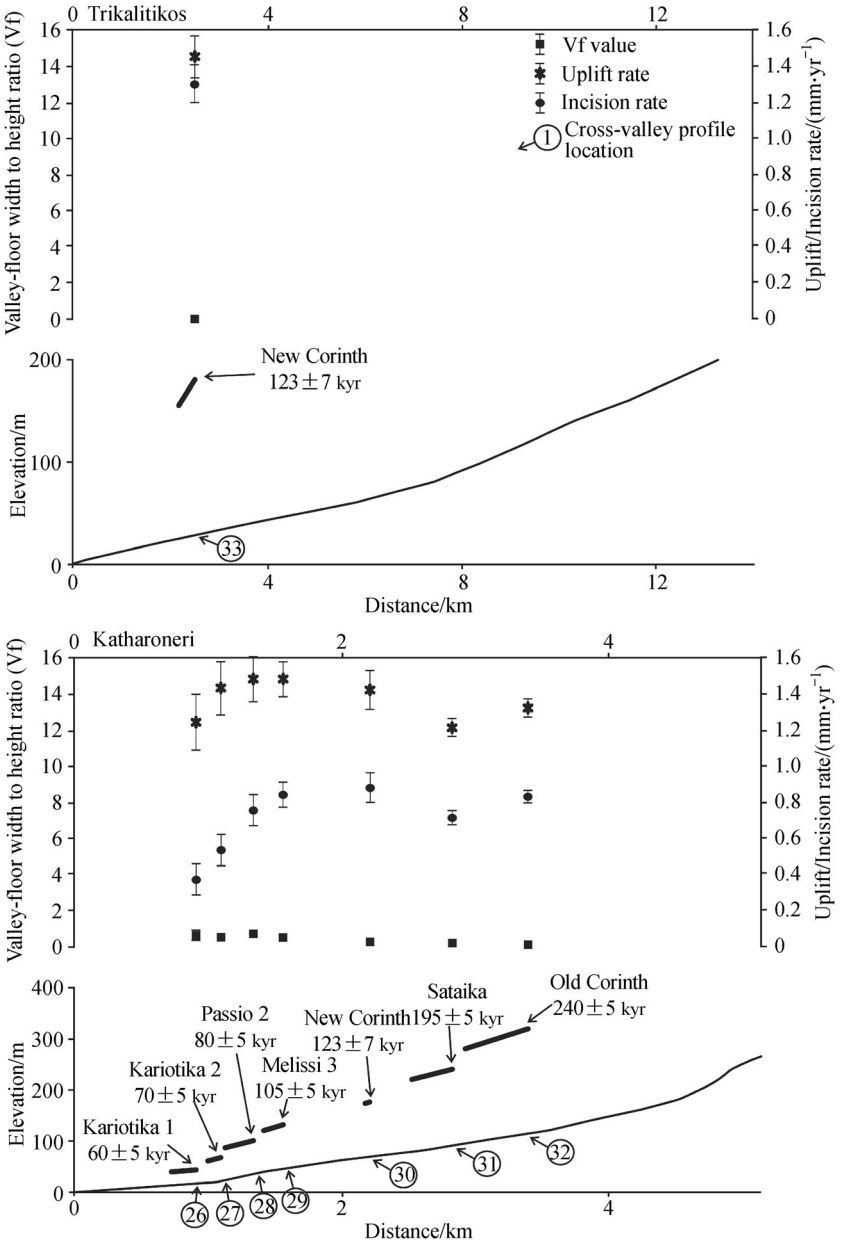


**Fig. 10** Longitudinal profiles of the lower reaches of the modern Katharoneri and Trikalitikos stream beds. Profiles of marine terrace surfaces along the west bank of the stream channels are also depicted. The name and the age of each marine terrace are given. Arrows indicate the locations of the inner edges of the marine terraces. Numbers in circles correspond to the locations and the numbers of the valley-cross profiles of Fig. 6 used for the estimation of long-term stream incision rates. Diagrams above longitudinal profiles show rock uplift rates, the ratio of valley floor width to valley height (Vf), and fluvial incision rates for the streams estimated from the valley-cross profiles. Right axis is the calculated uplift and incision rates; left axis is the parameter of valley floor width to valley height (Vf).

reaches of the streams. Thus Vf is a morphometric variable which can be used to infer incision activity in the study area.

### 4.4 Long-term rock uplift rates

The calculated long-term uplift rates range from 0.4±0.02 mm/yr to 1.49±0.12 mm/yr (Table 2, Fig. 15). The highest rate has been estimated along the Katharoneri stream for the period of the last 105±5 kyr whereas the lowest rock uplift rate is observed along the Xerias river for the last 310±5 kyr. Rock uplift is strongly dependent on the distance of the cross-valley profiles' locations from the Xylokastro fault trace (Fig. 15) as is shown by the negative value of the correlation coefficient obtained (−0.94). This very strong relationship is described by the following

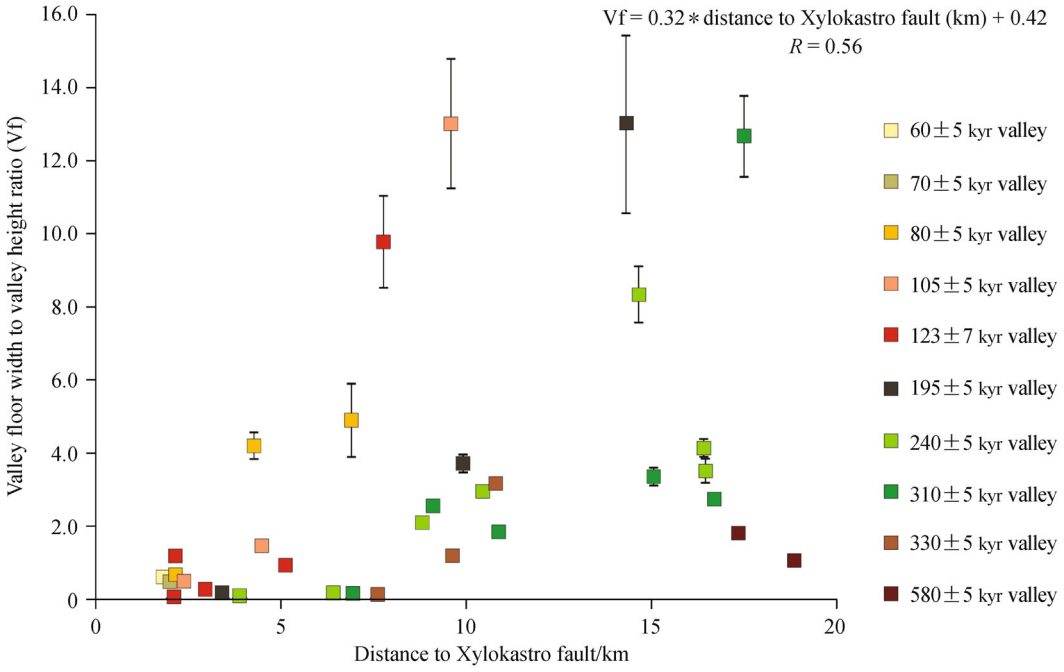


**Fig. 11** Plot of ratio of valley floor width to valley height (Vf), estimated at selected locations along the stream channels from valley-cross profiles, as a function of distance from the Xylokastro fault trace.

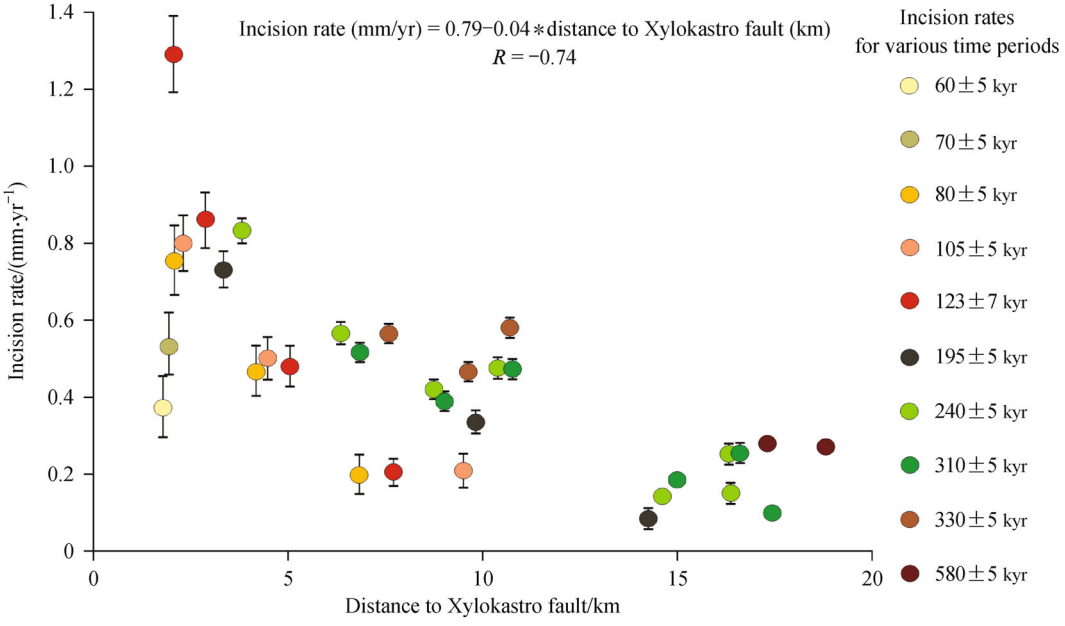


**Fig. 12** Plot of long-term incision rates estimated at selected locations along the stream channels from valley-cross profiles, as a function of distance from the Xylokastro fault trace. Different colors of the points correspond to mean incision rates estimated for various time periods.

equation:

$$\text{Uplift rate (mm/yr)} = 0.072 * \text{distance to Xylokastro fault (km)} + 1.56$$

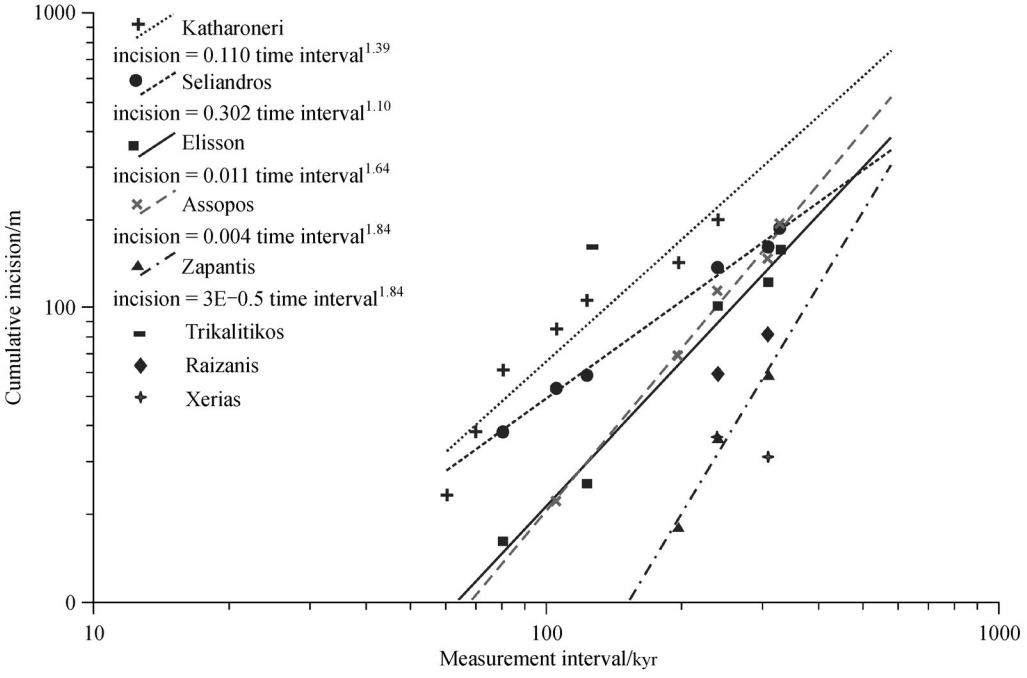


**Fig. 13** Log-log plot of cumulative incision (in m) vs. measurement interval (ka). Regression lines and power law functions that describe this relation for the streams of the study area are also given.

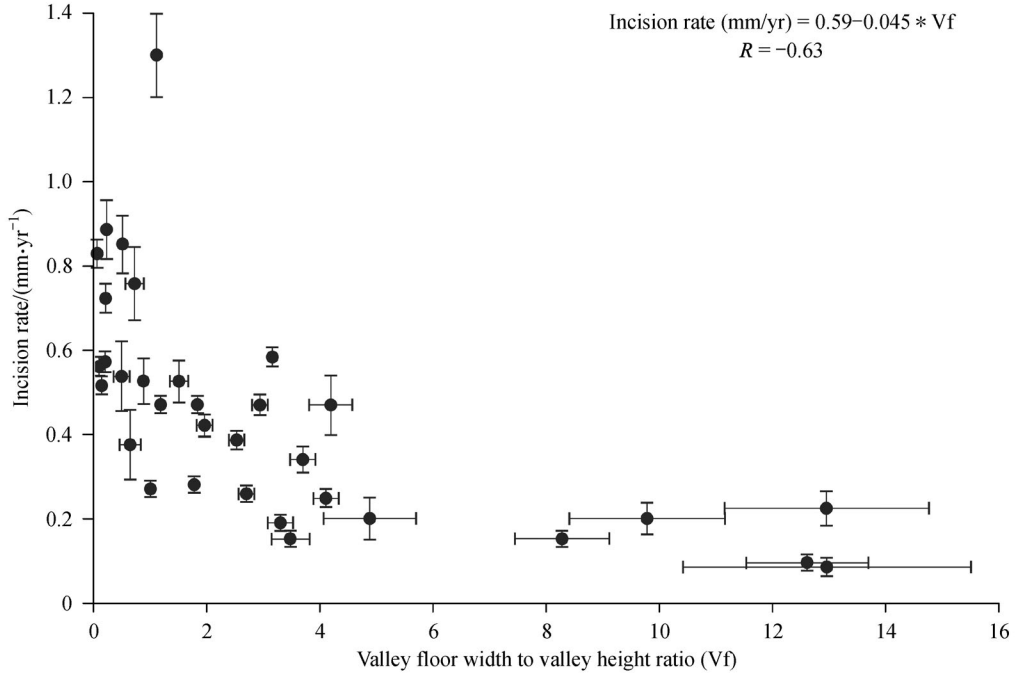


**Fig. 14** Ratio of valley floor width to valley height (Vf) vs. mean stream incision rates for thirty-three locations along the main channels of the studied streams.

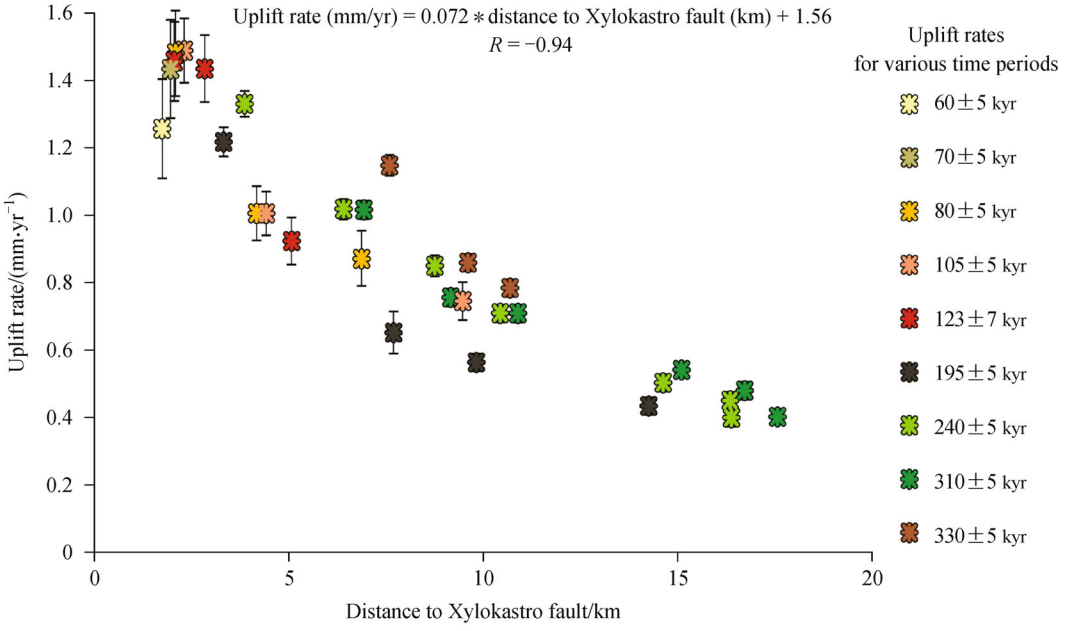


**Fig. 15** Plot of long-term rock uplift rates estimated at the locations of the valley-cross profiles, as a function of the distance from the Xylokastro fault trace. Different colors of the points correspond to mean rock uplift rates estimated for various time periods.

The geographic distribution of rock uplift rates with higher values at the western part of the area and gradually lower values towards the east indicates that uplift is primarily caused by the Xylokastro fault footwall flexure.

There is a very strong relationship among rock uplift and fluvial incision. The plot of rock uplift rates vs. fluvial incision rates is indicative of this very strong positive relation (correlation coefficient: 0.84) (Fig. 16). These variables are connected with the following equation:

$$\text{Incision rate (mm/yr)} = 0.635 * \text{uplift rate (mm/yr)} - 0.11$$

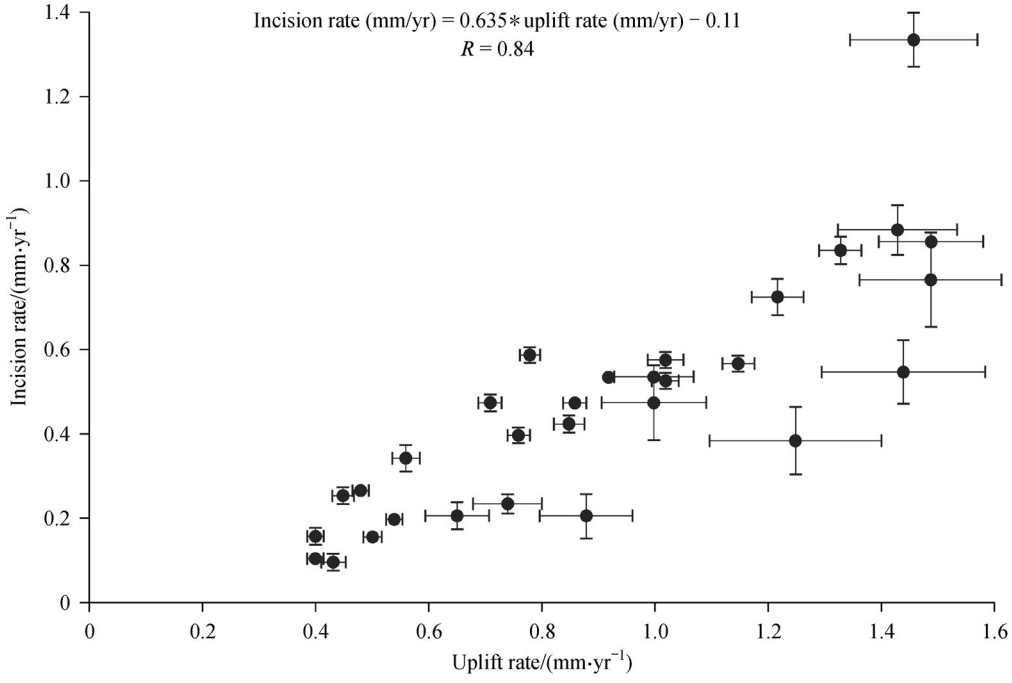


**Fig. 16** Rock uplift rates vs. stream incision rates for thirty-one locations along the main channels of the studied streams.

This relation suggests that tectonic uplift exerts an important control on fluvial incision in the study area. The correlation is very strong partly due to lithological similarities of the geological formations of the locations where these rates were estimated.

### 4.5 Stream Power estimations

In order to investigate the spatial variation of stream power along the channels and its possible relation with long-term mean fluvial incision rates, the Stream Power Index (SI) which describes the potential flow erosion at a given point of the stream channel was estimated at the locations of cross-valley profiles (Table 2). The values of the index range between 5.14 and 6.25. The lower value is estimated 0.9 km upstream from the mouth of the Katharoneri stream while the highest values correspond to locations along the main channel of the Assopos River, which has the more extensive basin among the streams of the study area. In general, stream power decreases towards the downstream side of the channel (Knighton, 1999). This may be the result of loss of kinetic energy while travelling through reaches of lower gradient. Such decrease is observed for the channels of the Raizanis, Elisson, and Seliandros. A positive correlation exists between stream power index and long-term incision rates for these streams. For the other rivers a relatively constant stream power index value is estimated along the lower reaches. For all the studied rivers, stream power seems to be strongly controlled by the local channel slope since no significant tributaries contribute to the upslope basin area.

## 5 Conclusions

In this study the evaluation of long-term stream incision rates on the uplifted block of the Xylokastro normal fault, in north Peloponnese, over the last 580±5 kyr is attempted. Rates of incision were calculated along the lower reaches of eight streams that cut down through the footwall of the Xylokastro fault. A series of ten uplifted late Pleistocene marine terraces, in amphitheatric form due to the activity of the offshore Xylokastro fault, which have been previously correlated with the worldwide chronology of glacio-eustatic sea-level highstands in the last 580±5 kyr, provided us with a unique set of interglacial sea-level highstands markers (palaeo-horizontal lines originally at sea-level) to estimate precise long-term rock uplift rates as well as downcutting along the streams.

We estimated fluvial incision using an accurate (2 m× 2 m) DEM produced by detailed topographic maps of 1:5,000 scale with a horizontal and vertical accuracy of ±1 m. Our approach involves precise quantitative estimation of rock uplift rates and fluvial incision rates for all nine marine terraces. Furthermore, the shape of the stream valleys is investigated by estimating the ratio of valley floor width to valley height for valleys of given ages but also for different distances from the Xylokastro fault. The relationship between incision rate value estimates and values of the ratio of valley floor width to valley height was also investigated.

The geomorphic evolution of the studied valleys has been affected by the lithology of the bedrock, sea level fluctuations during the late Quaternary, and mainly due to the head-ward erosion and incision of the channels caused by the tectonic uplift of the area. Values of valley floor width to valley height ratio (Vf) within the study area range between 0.10±0.01 and 13.00±2.49 and differ in magnitude between different locations. Variations of Vf values indicate significant difference in the valley shapes between the streams of the eastern and western parts of the study area. The spatial distribution of the Vf ratio and stream incision are strongly controlled by the distance of the valleys from the active Xylokastro fault. The lowest Vf values ($<1.00$), which imply more intense bedrock incision, were estimated for the streams which drain the western part of the study area (Trikalitiko, Katharoneri, and Seliandros). This is the consequence of rapid down-cutting resulting from higher rates of tectonic uplift since these streams drain an area closer to the trace of the Xylokastro normal fault. On the other hand streams of the eastern part (which are located far from the fault) are characterized by significantly higher Vf values. Higher values were observed at the lower reaches of the streams, whereas lower values resulted from the incised reaches of the streams especially at their paths through the older and higher marine terraces.

Long-term channel incision rates on the footwall of the fault decrease with distance from the trace of the Xylokastro fault. Incision is strongly controlled by the distance of the stream valleys from the fault trace as evidenced by the value of the correlation coefficient obtained ($-0.74$). The highest incision rate (1.14±0.1 mm/yr for the last 123±7 kyr) was estimated for the westernmost stream (Trikalitikos) while the lower incision rate (0.10±0.01 mm/yr for the last 310±5 kyr) corresponds to Xerias Stream which is located eastwards about 17.5 km from the fault. Similarly high uplift rates (higher than 1.3 mm/yr) were estimated for the terraces located at the extreme western part of the study area (about 5 km from the Xylokastro fault). On the other hand lower uplift rates of 0.40 mm/yr were observed for the terraces located east and far away (about 18 km from the fault trace). For most of the streams, downcutting rates increase slightly with the age and elevation of the terraces. Incision rate values along the Xerias, Assopos, Elisson, and Seliandros streams show a decrease of mean downcutting for the 310±5 kyr terrace. This is attributed to the occurrence of a much thicker, more resistant to fluvial erosion caprock consisting of well cemented sands and conglomerates on top of this marine terrace.

On the other hand a long-term relative stability of river

incision rate over the last 580±5 kyr has been observed along the main stream channels of the Seliandros, Elisson, Raizanis, and Zapantis. Stream incision must have accelerated during glacial epochs due to lowering of base level whereas during interglacial periods downcutting must have been slower since tectonic uplift was the only cause of incision. The geographic distribution of fluvial incision rates indicates that local uplift in the footwall of the Xylokastro fault is the main controlling factor of both morphology of the valleys and downcutting. Long-term fluvial incision within the study area is in close agreement with long-term uplift. This very strong positive relationship suggests that tectonic uplift due to fault footwall flexure exerts an important control on fluvial incision. Average uplift rates have been three times higher south of Xylokastro, near the fault, than south of Corinth, 15 – 20 km away from the fault trace, while average incision rates have been four to five times higher south of Xylokastro than south of Corinth. We must mention here that changes in the rate of incision exist in nature due to changes in base level imposed by rock uplift paired with eustasy. Hence, stream incision is an unsteady process disturbed by episodes of aggradation and the streambeds' elevation oscillate through time. During the glacial periods the base-level was very low and the incision rates were much higher than during the interglacial periods.

A strong relationship between steam downcutting and the shape of the valleys is concluded by the comparison of the ratio of valley floor to valley height values with mean incision rate estimates (correlation coefficient: – 0.63). This relation is partly controlled by the lithological similarities of the geological formations along the lower reaches of the streams.

Stream Power Index values decreases downstream for the channels of the Raizanis, Elisson, and Seliandros. A positive correlation exists between stream power index and long-term incision rates for these streams while a relatively constant stream power index value is estimated along the lower reaches of the other rivers.

**Acknowledgements** We would like to thank the editors of the journal and three anonymous reviewers for their helpful suggestions, comments, and corrections that significantly improved the manuscript.

## References

Ambraseys N, Jackson J (1997). Seismicity and strain in the Gulf of Corinth (Greece) since 1694. J Earthquake Eng, 1(3): 433–474

Armijo R, Meyer B, King G, Rigo A, Papanastassiou D (1996). Quaternary evolution of the Corinth Rift and its implications for the Late Cenozoic evolution of the Aegean. Geophys J Int, 126(1): 11–53

Avallone A, Briole P, Agatza-Balodimou A M, Billiris H, Charade O, Mitsakaki C, Nercessian A, Papazissi K, Paradissis D, Veis G (2004). Analysis of eleven years of deformation measured by GPS in the Corinth Rift Laboratory area. C R Geosci, 336(4 – 5): 301–311

Bell R E, McNeil L C, Bull J M, Henstock T J, Collier R E L, Leeder M R (2009). Fault architecture, basin structure and evolution of the Gulf of Corinth Rift, central Greece. Basin Res, 21(6): 824–855

Briole P, Rigo A, Lyon-Caen H, Ruegg J C, Papazissi K, Mitsakaki C, Balodimou A, Veis G, Hatzfeld D, Deschamps A (2000). Active deformation of the Corinth Rift, Greece: results from repeated Global Position System surveys between 1990 and 1995. J Geophys Res Solid Earth, 105(B11): 25606–25626

Brocard G Y, van der Beek P A, Bourles D L, Siame L L, Mugnier J L (2003). Long-term fluvial incision rates and postglacial river relaxation time in the French Western Alps from $^{10}$Be dating of alluvial terraces with assessment of inheritance, soil development and wind ablation effects. Earth Planet Sci Lett, 209(1 – 2): 197–214

Bull W B, McFadden L D (1977). Tectonic geomorphology north and south of the Garlock Fault, California. In: Doehring D O, ed. Geomorphology in Arid Regions. New York: State University of New York, Binghamton, 115–138

Burbank D W, Anderson R S (2007). Tectonic Geomorphology. Chelsea: Blackwell Science

Carcaillet J, Mugnier J L, Koci R, Jouanne F (2009). Uplift and active tectonics of southern Albania inferred from incision of alluvial terraces. Quat Res, 71(3): 465–476

Chappell J, Shackleton N J (1986). Oxygen isotopes and sea-level. Nature, 324(6093): 137–140

Chousianitis K, Ganas A, Gianniou M (2013). Kinematic interpretation of present-day crustal deformation in central Greece from continuous GPS measurements. J Geodyn, 71: 1–13

Clarke P J, Davies R R, England P C, Parsons B, Billiris H, Paradissis D, Veis G, Cross P A, Denys P H, Ashkenazi V, Bingley R, Kahle H G, Muller M V, Briole P (1998). Crustal strain in central Greece from repeated GPS measurements in the interval 1989–1997. Geophys J Int, 135(1): 195–214

Collier R E L (1990). Eustatic and tectonic controls upon Quaternary coastal sedimentation in the Corinth Basin, Greece. J Geol Soc London, 147(2): 301–314

Collier R E L, Leeder M R, Rowe R J, Atkinson T C (1992). Rates of tectonic uplift in the Corinth and Megara basins, Central Greece. Tectonics, 11(6): 1159–1167

Corbi F, Fubelli G, Luca F, Muto F, Pelle T, Robustelli G, Scarciglia F, Dramis F (2009). Vertical movements in the Ionian margin of the Sila Massif (Calabria, Italy). Italian Journal of Geosciences, 128(3): 731–738

Cucci L (2004). Raised marine terraces in the Northern Calabrian Arc (Southern Italy): a ~ 600 kyr-long geological record of regional uplift. Ann Geophys, 47(4): 1391–1406

Demoulin A, Beckers A, Hubert-Ferrari A (2015). Patterns of Quaternary uplift of the Corinth rift southern border (N. Peloponnese, Greece) revealed by fluvial landscape morphometry. Geomorphology, 246: 188–204

Deperet C (1913). Observations sur l' historique Pliocene et Quaternaire du golfe et de l' isthme de Corinthe. Comptes Rendus de l'Académie des Sciences Paris, 156: 1048–1052

Doutsos T, Piper D J W (1990). Listric faulting, sedimentation, and morphological evolution of the Quaternary eastern Corinth rift, Greece: first stages of continental rifting. Geol Soc Am Bull, 102(6): 812–829

Dufaure J J, Zamanis A (1980). Styles néotectoniques et étagements de niveaux marins sur un segment d'arc insulaire, le Péloponnèse, In: Proccedings of the Conference Niveaux marins et Tectonique Quaternaire dans l'Aire Méditerranéenne. Paris: CNRS, 77–107

Finnegan N J, Hallet B, Montgomery D R, Zeilter P K, Stone J O, Anders A M, Yuping L (2008). Coupling of rock uplift and river incision in the Namche Barwa-Gyala Peri massif, Tibet. Geol Soc Am Bull, 120 (1/2): 142–155

Finnegan N J, Schumer R, Finnegan S (2014). A signature of transience in bedrock river incision rates over timescales of $10^4 - 10^7$ years. Nature, 505(7483): 391–394

Florinsky I V (2012). Digital Terrain Analysis in Soil Science and Geology. Amsterdam: Elsevier-Academic Press

Floyd M A, Billiris H, Paradissis D, Veis G, Avallone A, Briole P, McClusky S, Nocquet J M, Palamartchouk K, Parsons B, England P C (2010). A new velocity field for Greece: implications for the kinematics and dynamics of the Aegean. J Geophys Res, 115(B10 B10403): B10403

Ford M, Rohais S, Williams E, Bourlange S, Jousselin D, Backert N, Malartre F (2013). Tectono-sedimentary evolution of the western Corinth rift (Central Greece). Basin Res, 25(1): 3–25

Freyberg B (1973). Geologie des Isthmus von Korinth. Erlanger Geologische Abhandlungen, 95: 1–183

Gaki-Papanastassiou K, Karymbalis E, Papanastassiou D, Maroukian H (2009). Quaternary marine terraces as indicators of neotectonic activity of the Ierapetra normal fault SE Crete (Greece). Geomorphology, 104(1 – 2): 38–46

Gallen S F, Pazzaglia F J, Wegmann K W, Pederson J L, Gardner W (2015). The dynamic reference frame of rivers and apparent transience in incision rates. Geology, 43(7): 623–626

Gardner T W, Jorgensen D W, Shuman C, Lemieux C R (1987). Geomorphic and tectonic process rates: effects of measured time interval. Geology, 15(3): 259–261

Harbor D J (1998). Dynamic equilibrium between an active uplift and the Sevier River, Utah. J Geol, 106(2): 181–194

Haviv I, Enzel Y, Whipple K X, Zilberman E, Matmon A, Stone J, Fifield K L (2010). Evolution of vertical knickpoints (waterfalls) with resistant caprock: insights from numerical modeling. Journal of Geophysical Research – Earth Surface, 115: F03028

IGME (1970). Geological map of Greece (1:50,000), Nemea sheet

IGME (1972). Geological map of Greece (1:50,000), Korinthos sheet

IGME (1982). Geological map of Greece (1:50,000), Kandhila sheet

IGME (1983). Geological map of Greece (1:500,000)

IGME (1989). Geological map of Greece (1:50,000), Xylokastro sheet

Jackson J A, Gagnepain J, Houseman G, King G C P, Papadimitriou P, Soufleris C, Virieux J (1982). Seismicity, normal faulting and the geomorphological development of the Gulf of Corinth (Greece): the Corinth earthquakes of February and march 1981. Earth Planet Sci Lett, 57(2): 377–397

Kale V S, Shejwalkar N (2008). Uplift along the western margin of the Deccan Basalt Province: is there any geomorphometric evidence? J Earth Syst Sci, 117(6): 959–971

Katsafados P, Kalogirou S, Papadopoulos A, Mavromatidis E (2009). Cartographic representation of climate spatial variability in Greece. In: Proccedings of the 9th Symposium on Oceanography and Fishery. Patras: HCMR, 439–444

Keller E A, Pinter N (1996). Active Tectonics: Earthquakes Uplift and Landscapes. New Jersey: Prentice Hall

Keraudren B, Sorel D (1987). The terraces of Corinth (Greece) – A detailed record of eustatic sea-level variations during the last 500,000 years. Mar Geol, 77(1 – 2): 99–107

Kershaw S, Guo L (2001). Marine notches in coastal cliffs: indicators of relative sea-level change, Perachora Peninsula, central Greece. Mar Geol, 179(3 – 4): 213–228

Kirby E, Whipple K X (2012). Expression of active tectonics in erosional landscapes. J Struct Geol, 44: 54–75

Knighton D (1999). Downstream variation in stream power. Geomorphology, 29(3 – 4): 293–306

Koukouvelas I, Katsonopoulou D, Soter S, Xypolias P (2005). Slip rates on the Helike Fault, Gulf of Corinth, Greece: new evidence from geoarchaeology. Terra Nova, 17(2): 158–164

Kraal R (1999). Bedrock incision and knickpoint processes in streams along an uplifting coast, southern Península de Nicoya, Costa Rica. In: Mendelson C V, Mankiewicz C, eds. Proceedings Twelfth Keck Research Symposium in Geology. Northfield, Minnesota: Keck Geology Consortium, 188–191

Lavé J, Avouac J P (2001). Fluvial incision and tectonic uplift across the Himalayas of central Nepal. J Geophys Res Solid Earth, 106(B11): 26561–26591

Leeder M R, McNeill L C, Collier R E L, Portman C, Rowe P J, Andrews J E, Gawthorpe L (2003). Corinth rift margin uplift: new evidence from Late Quaternary marine shorelines. Geophysical Research Letters, 30/12: 13-1 –13-4

Leeder R, Mark F, Gawthorpe L, Kranis H, Loveless S, Pedentchouk N, Skourtsos E, Turner J, Andrews E, Stamatakis M (2012). A "Great Deepening": chronology of rift climax, Corinth rift, Greece. Geology, 40(11): 999–1002

Leeder R, Portman C, Andrews E, Collier R, Finch E, Gawthorpe L, McNeill L, Pérez-Arlucea M, Rowe P (2005). Normal faulting and crustal deformation, Alkyonides Gulf and Perachora peninsula, eastern Gulf of Corinth rift, Greece. J Geol Soc London, 162(3): 549–561

Leland J, Reid M R, Burbank D W, Finkel R, Caffee M (1998). Incision and differential bedrock uplift along the Indus River near Nanga Parbat, Pakistan Himalaya, from $^{10}$Be and $^{26}$ Al exposure age dating of bedrock straths. Earth Planet Sci Lett, 154(1 – 4): 93–107

Maroukian H, Gaki-Papanastassiou K, Karymbalis E, Vouvalidis K, Pavlopoulos K, Papanastassiou D, Albanakis K (2008). Morphotectonic control on drainage network evolution in the Perachoora Peninsula, Greece. Geomorphology, 102(1): 81–92

Maroukian H, Gaki-Papanastassiou K, Papanastassiou D (1997). Coastal changes in thebroader area of Corinth, Greece. American School of Oriental Research. Archaeol Rep, 04: 217–226

Marquardt C, Lavenu A, Ortlieb L, Godoy E, Comte D (2004). Coastal neotectonics in Southern Central Andes: uplift and deformation of marine terraces in Northern Chile (27?S). Tectonophysics, 394(3 – 4): 193–219

McNeill L C, Collier R E L (2004). Uplift and slip rates of the eastern Eliki fault segment, Gulf of Corinth, Greece, inferred from Holocene and Pleistocene terraces. J Geol Soc London, 161(1): 81–92

Merritts D, Bull W B (1989). Interpreting Quaternary uplift rates at the Mendocino triple junction, northern California, from uplifted marine

terraces. Geology, 17: 1020–1024

Merritts D, Vincent K R (1989). Geomorphic response of coastal streams to low, intermediate, and high rates of uplift, Medocino triple junction region, northern California. Geol Soc Am, 101(11): 1373–1388

Merritts D, Vincent K, Wohl E E (1994). Long river profiles, tectonism, and eustacy: a quide to interpreting fluvial terraces. J Geophys Res, 99(B7): 14,031–14,050

Morewood N, Roberts G (1999). Lateral propagation of the surface trace of the south Alkyonides normal fault segment, central Greece: its impact on models of fault growth and displacement–length relationships. J Struct Geol, 21(6): 635–652

Murray-Wallace C V, Woodroffe C D (2014). Quaternary Sea-Level Changes: A Global Perspective. New York: Cambridge University Press

Palyvos N, Mancini M, Sorel D, Lemeille F, Pantosti D, Julia R, Triantaphyllou M, De Martini P (2010). Geomorphological, stratigraphic and geochronological evidence of fast Pleistocene coastal uplift in the westernmost part of the Corinth Gulf Rift (Greece). Geol J, 45(1): 78–104

Papageorgiou S, Arnold M, Laborel J, Stiros S (1993). Seismic uplift of the harbour of ancient Aigeira, Central Greece. Int J Naut Archaeol, 22(3): 275–281

Pavlides S, Caputo R (2004). Magnitude versus faults' surface parameters: quantitative relationships from the Aegean Region. Tectonophysics, 380(3 – 4): 159–188

Pazzaglia F, Brandon M (2001). A fluvial record of long-term steady-state uplift and erosion across the Cascadia forearc high, western Washington State. Am J Sci, 301(4 – 5): 385–431

Pillans B (1990). Pleistocene marine terraces in New Zealand: a review. NZ J Geol Geophys, 33(2): 219–231

Pirazzoli P, Stiros S, Fontugne M, Arnold M (2004). Holocene and Quaternary uplift in the central part of the southern coast of the Corinth Gulf (Greece). Mar Geol, 212(1 – 4): 35–44

Proença Cunha P, Antunes Martins A, Daveau S, Friend P F (2005). Tectonic control of the Tejo river fluvial incision during the late Cenozoic, in Rodao-central Poerugal (Atlantic Iberian border). Geomorphology, 64(3 – 4): 271–298

Rigo A, Lyon-Caen H, Armijo R, Deschamps A, Hatzfeld D, Makropoulos K, Papadimitriou P, Kassaras I (1996). A microseismic study in the western part of the Gulf of Corinth (Greece): implications for large-scale normal faulting mechanisms. Geophys J Int, 126(3): 663–688

Robustelli G, Luca F, Corbi F, Pelle T, Dramis F, Fubelli G, Scarciglia F, Muto F, Cugliari D (2009a). Alluvial terraces on the Ionian coast od northern Calabria, southern Italy: implications for tectonic and sea level controls. Geomorphology, 106(3 – 4): 165–179

Robustelli G, Luca F, Corbi F, Fubelli G, Scarciglia F, Dramis F (2009b). Geomorphological map of the Ionian area between the Trionto and Colognati River catchments (Calabria, Italy). J Maps, 5 (1): 94–102

Rohais S, Eschard R, Guillocheau F (2008). Depositional model and stratigraphic architecture of rift climax Gilbert- type fan deltas (Gulf of Corinth, Greece). Sediment Geol, 210(3 – 4): 132–145

Rostami K, Peltier W R, Mangini A (2000). Quaternary marine terraces, sea-level changes and uplift history of Patagonia, Argentina: comparisons with predictions of the ICE-4G (VM2) model of the global process of glacial isostatic adjustment. Quat Sci Rev, 19 (14 – 15): 1495–1525

Sebrier M (1977). Tectonique récente d'une transversale a l'Arc Egéen: le Golfe de Corinthe et ses régions périphériques. Thèse 3eme cycle, Univ. Paris-Sud: France

Seong Y B, Owen A, Bishop M P, Bush A, Clendon P, Copland L, Finkel R C, Kamp U, Shroder J F Jr (2008). Rates of fluvial bedrock incision within an actively uplifting orogen: Central Karakoram Mountains, northern Pakistan. Geomorphology, 97(3 – 4): 274–286

Stewart I S (1996). Holocene uplift and palaeoseismicity on the Eliki fault, western gulf of Corinth. Ann Geofis, 39: 575–588

Stewart S, Vita-Finzi C (1996). Coastal uplift on active normal faults: the Eliki Fault, Greece. Geophys Res Lett, 23(14): 1853–1856

Syndera N P, Whipple K X, Tucker G E, Merritts D J (2003). Channel response to tectonic forcing: field analysis of stream morphology and hydrology in the Mendocino triple junction region, northern California. Geomorphology, 53(1 – 2): 97–127

Turner J A, Leeder M R, Andrews J E, Rowe P J, Van Calsteren P, Thomas L (2010). Testing rival tectonic uplift models for the Lechaion Gulf in the Gulf of Corinth rift. J Geol Soc London, 167(6): 1237–1250

Valensise G, Pantosti D (1992). A 125 kyr-long geological record of seismic source repeatability: the Messina Straights (southern Italy) and the 1908 earthquake (Ms 7.5). Terra Nova, 4(4): 472–483

Vita-Finzi C, King G C P (1985). The seismicity, geomorphology and structural evolution of the Corinth area of Greece. Philos Trans R Soc Lond, 314(1530): 379–407

Wakabayashi J, Sawyer T (2001). Stream incision, tectonics, uplift, and evolution of topography of the Sierra Nevada, California. The Journal of Geology, 109: 539–562

Westeway R (2002). The Quaternary evolution of the Gulf of Corinth, central Greece: coupling between surface processes and flow in the lower continental crust. Tectonophysics, 348: 269–318

Whipple K X (2001). Fluvial landscape response time: how plausible is steady-state denudation? Am J Sci, 301(4 – 5): 313–325

Whipple K X, Tucker G E (1999). Dynamics of the stream power river incision model: implications for height limits of mountain ranges, landscape response timescales, and research needs. J Geophys Res, 104(B8): 17661–17674

Zazo C, Goy J L, Dabrio C J, Bardají T, Hillaire-Marcel C, Ghaleb B, González-Delgado J Á, Soler V (2003). Pleistocene raised marine terraces of the Spanish Mediterranean and Atlantic coasts: records of coastal uplift, sea-level highstands and climate changes. Mar Geol, 194(1–2): 103–133

## AUTHOR BIOGRAPHIES

Efthimios Karymbalis holds a BSc degree in Geology from the National and Kapodistrian University of Athens, Greece (1992). He also holds a PhD degree in Geomorphology from the same University (1996).

He is an ASSOCIATE PROFESSOR in Coastal and Fluvial Geomorphology at the Department of Geography of the Harokopio University of Athens, Greece. He has

published a lot of papers in peer reviewed international scientific journals like Geomorphology, Journal of Coastal Research, Zeitschrift fur Geomorphologie, Geological Society of America Special Publications, etc. and numerous papers in Proceedings of International Conferences. His research interests include Coastal and Fluvial Geomorphology, Geomorphological Mapping, Quantitative Geomorphometry, Natural Hazards (flash floods, sea-level rise).

Prof. Karymbalis is member of the executive committee of the Geomorphological Society of Greece, member of many national (such as the Geological Society of Greece, Hellenic Geographical Society) and International Scientific Societies (Geological Society of South Africa, European Geosciences Union).

E-mail: karymbalis@hua.gr

Dimitrios Papanastassiou holds a BSc degree in Geology from the National and Kapodistrian University of Athens, Greece (1975). He also holds an MSc degree in Seismology and Earthquake Engineering from the International Institute of Seismology and Earthquake Engineering, Government of Japan (1986) and a PhD degree in Seismology from the University of Athens, Greece (1989).

He is a RESEARCH DIRECTOR at the Institute of Geodynamics of the National Observatory of Athens, Greece. In the past he worked as a Geologist at the Department of Hydrogeology, Institute of Geology and Mining Research of Greece (1980). He has published quite a lot (more than 70) papers in peer reviewed international scientific journals (with more than 1200 citations) and about 90 papers in Proceedings of International Conferences. His research interests include Seismology, Seismic Arrays, Active Tectonics, Morphotectonics, Seismotectonics, Palateseismology.

Dr. Papanastassiou serves as a reviewer for multiple earth science journals.

E-mail: d.papan@gein.noa.gr

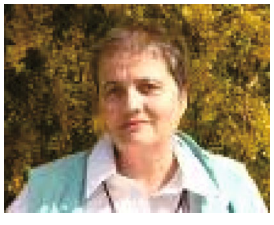

Kalliopi Gaki-Papanastassiou holds a BSc degree in Geology from the National and Kapodistrian University of Athens, Greece (1978). She also holds an MSc degree in Oceanography (1983) and a PhD degree in Geomorphology (1991) from the same University.

She is a PROFESSOR in Geomorphology at the Department of Geography-Climatology, Faculty of Geology-Geoenvironment, National and Kapodistrian University of Athens. She has more than 170 publications in peer reviewed international scientific journals and Proceedings of International Conferences. Her research interests include Coastal Geomorphology Fluvial Geomorphology, Morphotectonics, Quaternary Geology, Geoarchaeology, Natural Hazards and Environmental Geomorphology.

Prof. Gaki-Papanastassiou is the secretary of the executive committee of the Geomorphological Society of Greece. She is a member of many other ational (such as the Geological Society of Greece, Hellenic Geographical Society) and International Scientific Societies (International Association of Geomorphologists, European Geosciences Union).

E-mail: gaki@geol.uoa.gr

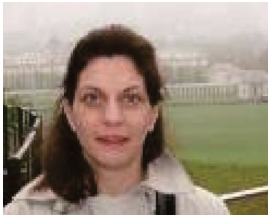

Maria Ferentinou holds a BSc in Geology from the University of Patras, Greece and a PhD in Engineering Geology from the National Technical University of Athens, Greece (2004).

She worked as Postgraduate Researcher in Landslide Hazard (2004 – 2008) while in 2009 she was appointed Adjunct Lecturer in the Department of Geography in Harokopio University. Since 2003 she is SENIOR LECTURER at the Department of Geology of the KwaZulu Natal University, Durban, South Africa. She has a lot of publications in peer reviewed international scientific journals and Proceedings of International Conferences. Her research interests include soil and rock slope stability, engineering geology, landslide mechanics and landslide hazard, GIS in the context of Earth Sciences, and artificial intelligence in Earth Sciences.

Dr. Ferentinou is member of many National (such as the Geological Society of Greece, Hellenic Scientific Society of Soil Mechanics, Hellenic Society of GIS) and International (International Society for Soil Mechanics and Geotechnical Engineering, International Society for Rock Mechanics) Scientific Societies.

E-mail: Ferentinou@ukzn.ac.za

Christos Chalkias holds a BSc degree in Geology from the National and Kapodistrian University of Athens, Greece (1991). He also holds a PhD degree in Physical Geography-Geoinformatics from the same University (1996).

He is an ASSOCIATE PROFESSOR in Geographic Information Systems and Applied Geography at the Department of Geography of the Harokopio University of Athens, Greece. Since 2003 he is Head of the Department. He has published a lot of papers in peer reviewed international scientific journals (among others Journal of Maps, Journal of Coastal Research, Zeitschrift fur Geomorphologie, Applied Geography) and numerous papers in Proceedings of International Conferences. His research interests include GIS, Applied Geography, Spatial analysis, Modeling of Natural Disasters.

Prof. Chalkias is member of many National (such as the Geological Society of Greece, Hellenic Geographical Society, Hellenic Society of GIS) and International Scientific Societies.

E-mail: xalkias@hua.gr